CHALMERS
UNIVERSITY OF TECHNOLOGY

Life cycle assessment of phase-change solvents for post-combustion CO_2 capture

Master's thesis in Sustainable Energy Systems

Maja GUSTAFSSON
Thibaud ROSIN

Department of Space, Earth and Environment
CHALMERS UNIVERSITY OF TECHNOLOGY
Gothenburg, Sweden 2019

Master's thesis 2019-01:2019-06

Modelling of synthesis process and life cycle assessment of phase-change solvents used for post-combustion CO_2 capture (non-confidential)

Maja GUSTAFSSON, Thibaud ROSIN

CHALMERS
UNIVERSITY OF TECHNOLOGY

Department of Space, Earth and Environment
Division of environment
Chalmers University of Technology
Gothenburg, Sweden 2019

Modelling of production processes and cradle-to-gate life cycle assessment of phase-changing solvents used for post-combustion CO_2 capture (non-confidential)

Supervisor: Gulnara Shavalieva, Department of Space, Earth and Environment
Examiner: Stavros Papadokonstantakis, Department of Space, Earth and Environment

Master's Thesis 2019-01:2019-06
Department of Space, Earth and Environment
Division of Environment
Chalmers University of Technology
SE-412 96 Gothenburg
Telephone +46 31 772 1000

Cover: Power Plant, Petr Kratochvil (publicdomainpictures.net)

Typeset in LaTeX
Gothenburg, Sweden 2019

Abstract

As climate change and global warming is one of the greatest challenges of the 21st century, several mitigation methods are under development. Post-combustion CO_2 capture and storage are one of the most mature industrial methods to capture and store CO_2. The capture includes the use of a CO_2 absorbing solvent. In the ROLINCAP project, several phase-changing solvents are under investigation. By using a phase-changing solvent, the energy requirement of the CO_2 capture has been proven to decrease.

However, while a lot of research is focused on finding new and improved solvents, the cradle-to-gate environmental impact of their production is unknown. During this study, this environmental impact of DMCA, MCA, MAPA and S1N, characteristic solvents exhibiting phase change behavior alone or in blends, have been investigated. DMCA and MCA can be used alone as phase-changing solvents.

A procedure was developed which enables the life-cycle-assessment of non-conventional, non-industrially produced chemicals. The method consisted of three main steps; (1) a literature study in order to find industrially suitable routes of synthesis for the compounds, (2) modelling the different manufacturing processes in Aspen Plus, and studying the impact of key parameters, and (3) using the results of the modelling to perform cradle-to-gate LCAs (looking at Cumulative Energy Demand, Global Warming Potential (100a) and total ReCiPe (H.A) indicators). By applying this method to the representative solvents mentioned above, an assessment of their environmental impact could be made.

It was found that the environmental impact of the MAPA production was the smallest, followed by S1N and DMCA, while the highest impact was MCA. However, the impact per captured tonne CO_2 could only be calculated for MCA, due to a lack of data for the other compounds. Thus no comparison between the compounds could be made.

The cradle-to-gate LCA also gives insights to what parts of the production processes are the most environmentally damaging. Thus, this study does not only provide data to bridge the gaps in the environmental foot print of post-combustion CO_2 capture processes based on characteristic phase-changing solvents, but is also very useful for further research on the environmentally weak points of process synthesis of such solvents.

Keywords: Life-Cycle-Assessment, LCA, Phase-Changing Solvents, Process Modelling, Solvent Manufacturing

Acknowledgements

Our acknowledgements goes to our supervisor Gulnara Shavalieva and examiner Stavros Papadokonstantakis, without whom the completion of this work would not have been possible. A special thanks also go to Cyril Barsu, Nina Kann and Derek Creaser for their help.

Maja Gustafsson and Thibaud Rosin, Gothenburg, June 2019

List of Abreviations

CA	Cyclohexylamine
CCS	Carbon Capture and Storage
CED	Cumulative Energy Demand
DMA	Dimethylamine
DMAPA	3-dimethylaminopropylamine
DMCA	N,N-dimethylcyclohexylamine
GHG	Greenhouse Gas
GWP	Global Warming Potential
IL	Ionic Liquid
LCA	Life Cycle Assessment
LCIA	Life Cycle Impact Assessment
LLE	Liquid-Liquid Equilibrium
MAPA	3-methylaminopropylamine
MCA	N-methylcyclohexylamine
MEA	Monoethanolamine
OVA	5-oxo-5-(pyridyl)valeric Acid
PCC	Post-Combustion Capture
VLLE	Vapour-Liquid-Liquid Equilibrium
WWT	Wastewater Treatment

Contents

List of Figures

List of Tables

1

Introduction

Climate change and global warming is one of the greatest challenges of the 21st century. Population growth and economics are forces that have been driving the greenhouse gas emissions during the last years to the highest levels in history [1]. The main cause of the human-induced global warming is the emissions of carbon dioxide (CO_2) from industries and combustion of fossil fuels [2]. Out of the total greenhouse gas emissions (calculated as CO_2-equivalents) in 2015, CO_2 accounted for 76% [3].

Carbon capture and storage (CCS) is a technology developed to reduce the CO_2 emissions from industries. As the name suggests, CCS involves first the capture of CO_2 and thereafter storage [2]. In 2018, 23 large-scale CCS facilities were in operation or under construction around the world [4]. The captured CO_2 is stored in deep geological storage, in depleted oil and gas reservoirs, unexploited coal seams and deep saline aquifers [5].

There are three main technologies available for the capture; pre-combustion capture, post-combustion capture, and oxyfuel capture [6], with the most mature technology being post-combustion capture. In post-combustion capture (see Figure 1.1), CO_2 is separated from the flue gases after the fuel combustion.

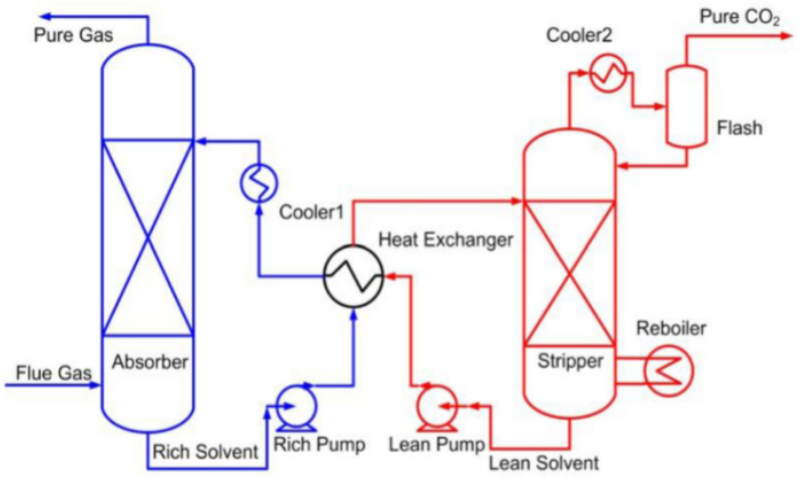

Figure 1.1: Basic CCS process set-up [7]

The solution used in the post-combustion CO_2 capture process is an amine solvent, and monoethanolamine (MEA) is the most commonly used. However, in such processes, there are many process parameters that have to be considered, such as solvent degradation, CO_2

loading capacity, corrosion and energy consumption during regeneration [8]. Therefore, a lot of research has been carried out trying to find better and more efficient solvents to use. One of the possible solutions for improvement explored in the ROLINCAP project [9] at the Division of Energy Technology at Chalmers is the use of phase-change solvents for CO_2 capture. Phase-change solvents have the capacity to form a liquid-liquid equilibrium (LLE) at certain temperatures and CO_2 concentrations. The CO_2-rich organic liquid phase can be separated from the CO_2-lean aqueous liquid phase by density differences prior to being sent to the stripper, therefore reducing its energy demand.

However, while a lot of research is focused on finding new solvents for more efficient and less expensive CCS, the environmental impacts of the new solvents are unknown. Since there is always a risk of solvent degradation and fugitive solvent losses even with the phase-change solvents, there might be a constant demand of solvent input into the CCS-process. In addition, there is a potential increase of the use of phase-change solvents worldwide, which would increase the production demand further. The impact of producing these solvents in large scale is therefore highly significant, from a life cycle perspective.

1.1 Purpose

The project focuses on the environmental impact of the manufacturing of four solvents; MCA, DMCA, MAPA and S1N. Their impacts are compared with the impact of MEA manufacturing, since MEA is currently well-known and industrially produced. In addition, the impacts are estimated using a FineChem estimation tool.

A cradle-to-gate life cycle assessment based on the energy and mass balances from the modelled production processes was performed, and compared to the estimated impacts. Both literature data and results from the process modelling was used to evaluate the impact of the processes in terms of Global Warming Potential, Cumulative Energy Demand and ReCiPe indicators.

S1N is a confidential compound. Therefore, appendices D through F are not included is this version of the report.

2

Background

2.1 Post-combustion carbon capture

The amine scrubbing technology used in post-combustion CO_2 capture was established for removing hydrogen sulphide and CO_2 from gas streams in the oil and chemical industries over 70 years ago [10]. The capture is done in two steps; absorption of the CO_2 and the regeneration of the solvent. The flue gases are led through an absorber, flowing from the bottom against a counter-current stream of an absorbing amine solvent. After the CO_2 in the flue gases are absorbed by the solvent, the rest of the flue gas leaves the top of the absorber. The CO_2 loaded solvent is thereafter led from the bottom of the absorber into the top of a stripper column, where the CO_2 is stripped from the solvent, and thereafter collected. The regenerated solvent led from the bottom of the stripper is recycled back to the absorber to be reused [11].

The concentration of CO_2 in the flue gases from combustion using air as the oxidant varies between about 4-14%, depending on the fuel. Due to the low concentration, the capturing equipment must be able to handle large volumes of gas, making it large and expensive [10]. One way to reduce the size of the absorber is to use a solvent with a high chemical reactivity with CO_2 [11].

Several compounds in the flue gases, such as sulphur dioxide, nitrous oxides and oxygen, can react with the amine solvents, forming substances such as heat stable salts [12]. This results in a degradation of the solvent, increasing the demand of solvent make-up. Different amine solvents have different affinities for such reactions, as well as for thermal degradation. In the presence of CO_2, it has been shown that tertiary-, cyclic-, and hindered primary amines are the most stable amines [13].

Another important factor is the energy requirement of the regeneration of the solvent. When the conventional MEA is used as the solvent, the absorber temperature is typically 40-60°C [12]. While the regeneration temperature in the stripper is about 100-120°C, resulting in the stripper reboiler having the main energy requirement in the process [12].

2.2 Phase-changing solvents

The main idea of using phase-changing solvents is to reduce the amount of energy required in the stripper by reducing the inlet flow rate. A liquid-liquid equilibrium (LLE) between water, CO_2 and certain amine solvents can be formed under certain operation conditions. When this occurs, one mostly organic CO_2-rich phase is formed along with one mostly aqueous CO_2-lean phase [14]. Only the CO_2-rich liquid phase is sent to the stripper, which reduces its energy requirement, and the lean phase can be sent back directly to the absorption column.

There are a lot of parameters to consider when assessing a phase-change solvent. These parameters include the capacity for CO_2 capture, the properties that may affect its fugitive losses (e.g. vapor tension), heat of regeneration, and the degradation tendency.

This project focused on four amines; the tertiary amine DMCA, the secondary amine MCA and the diamine MAPA (Figure 2.1), as well as S1N (included in the confidential Appendix D). All these amines present high or relatively high CO_2 loading capacities due to the multiple substitutions of the nitrogen atom. However, MAPA alone is not a phase-change solvent, but it is typically blended with phase-changing solvents because of its high CO_2 capture reaction rate.

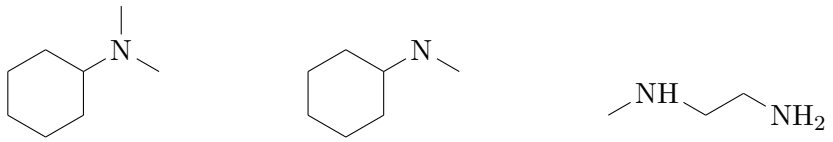

DMCA MCA MAPA

Figure 2.1: amines considered for a hypothetical blend used for CO_2 capture

Data from the ROLINCAP project show that 6-8 tonne MCA can capture 1 tonne CO_2, with a make-up flow rate requirement of 1.5-2.5 kg MCA per tonne captured [9]. Comparably, MEA requires 13-18 tonne to capture 1 tonne CO_2, with a make-up flow rate of 0.87-1.5 kg per tonne captured [15, 16]. The corresponding numbers for DMCA and MAPA are unknown. However, based on the solvent structures, the capacity of CO_2 capture could be assumed to be ranked as DMCA > MCA $\geq$ MAPA $\geq$ MEA.

Tertiary amines, such as DMCA, tend to have a higher loading capacity and a lower heat of regeneration than primary or secondary, such as MEA [17]. By using DMCA instead of MEA in the process, the rich solvent flow rate sent to the stripper could potentially be reduced, further reducing the energetic cost of the regeneration step [14]. However, primary and secondary amines have a higher kinetic of absorption than tertiary amines [14, 18]. Therefore, using a mix of these amines allows both high CO_2 loading capacity and high rate of reaction in the absorption column. For these reasons, it is worth to investigate the environmental impact of producing these molecules to fill in data gaps in cradle-to-gate assessment of the post-combustion CO_2 capture process.

3

Theory

3.1 Route of synthesis

One of the main challenges for the modelling part of the project was to find industrially applicable production processes for the compounds. For both MCA and DMCA, only patents describing batch manufacturing processes were found. This was mostly due to the fact that none of those two molecules possess any large-scale applications. Therefore, all the continuous models made for the production of DMCA and MCA, as well as MAPA, are using results coming from batch production processes. Moreover, for MAPA, no complete manufacturing process was found. Therefore, information from different publications had to be combined to come up with a route of synthesis.

3.1.1 N,N-Dimethylcyclohexylamine (DMCA)

Currently DMCA is mostly industrially produced through reductive alkylation of cyclohexanone and dimethylamine (Figure 3.1) [19, 20, 21]. The market for N-substituted cyclohexylamines, such as DMCA, is small, and they are generally manufactured in batch reactors [20].

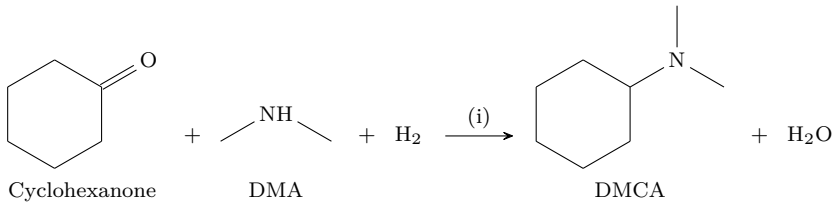

Figure 3.1: Formation of DMCA

Three patents describing the production of DMCA were found, all using different conditions (i). In a patent by Jackisch from 1985, the reaction occurs in a lab-scale batch reactor. The patent shows that the process when using a 5% palladium-on-carbon-catalyst resulted in a yield of 84-99.7% DMCA, with a conversion up to 100% [21]. The byproducts formed were cyclohexanol and dimethylaniline, and the product reached a purity up to 97.6 mol% DMCA [21]. The patent by Jackisch was however not further used in this study due to the numerous byproducts.

A patent by Efner et al. from 1990, also describes the reaction in a lab-scale batch reactor. By using a Raney copper catalyst, the conversion of cyclohexanone is reported to be 53-100%, depending on the reaction conditions. In the patent, acetic acid is used as a condensation promoter in order to facilitate the alkylation. The acetic acid was stated to promote both an increase of the cyclohexanone conversion into the desired product and an decrease of the percentage of formed byproduct cyclohexanol [22], resulting in low traces of cyclohexanol being the only byproduct. The patent states that a purity over 99 mol% DMCA can be reached after separation by distillation [22].

Moreover, a patent by Eberhardt et al. from 2009, describes the reaction in a continuous reactor in liquid phase. This process uses a fixed bed silver-and-palladium-on-silicon dioxide catalyst, reporting a conversion of cyclohexanone of 94-98% [23], depending on the reaction conditions. The patent reported the formation of cyclohexanol and MCA as byproducts, and a purity of up to 98 mol% DMCA [23]. The patent by Eberhardt et al. was not used further in the study due to the rare earth metal used in the catalyst, which would be unsuitable to use in an industrial scale. However, due to it describing a continuous process with yields and conversions similar to the ones described in the batch process by Efner, it supported the assumption that the patent by Efner could be used as a base for a continuous process.

3.1.2 N-methylcyclohexylamine (MCA)

MCA can be produced using a method similar to the method of producing DMCA; alkylation of cyclohexanone using methylamine (Figure 3.2). The cyclohexanone and methylamine first react to form an intermediate imine, which is then hydrogenated and forms MCA and water.

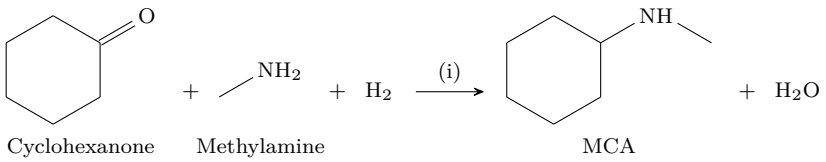

Figure 3.2: Formation of MCA

According to two Chinese patents, the production of MCA occurs in an aqueous solution, supported by a palladium-on-carbon or platinum-on-carbon catalyst ((i) in Figure 3.2). A patent from Chen et al. describes a process where an aqueous solution of 30 mass% methylamine is introduced in a batch reactor with almost pure cyclohexanone [24]. In the patent from Ji et al., an aqueous solution of 27 mass% methylamine is used [25]. In both these processes, the reaction occurs with pressurized hydrogen and yields are said to be excellent, up to 100% [25, 24].

The patents mostly differ by their separation steps. The patent by Chen et al. describes a separation of the remaining water and the organic phase using an addition of a solid base, and the patent by Ji et al. describes a separation using an addition of water soluble salts.

A paper by Brezina et al., provides an equilibrium constant for the the imine formation [26]. However, this constant did not correspond to any of the patented processes described above. As the experiment described did not take place under the same reaction conditions and no correlation between the constant and the reaction conditions was given, the constant could not be used during the modelling. No other equilibrium constants, or correlations providing equilibrium constants corresponding to temperature, were found during the literature study.

3.1.3 MAPA

An extensive literature found no description of the complete production of MAPA. However, a paper by Jiang et al. describes the formation of a nitrile compound by conjugate addition of methylamine and acrylonitrile. This nitrile compound can later be hydrogenated and form MAPA. The total reaction is shown in Figure 3.3.

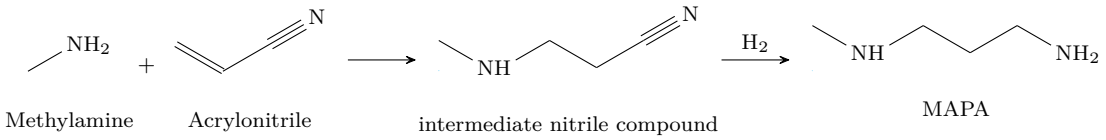

Figure 3.3: MAPA formation

The formation of the nitrile compound occur under solvent-free conditions, and the paper states a yield of 99% in room temperature with a reaction time of 5 minutes inside a batch reactor, without the formation of any byproducts [27]. The reaction is supported by an ionic liquid (IL) catalyst, shown in Figure 3.4.

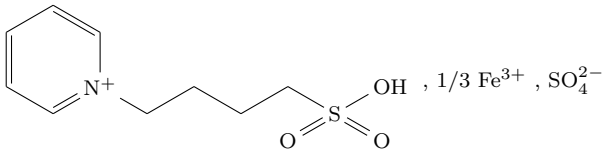

Figure 3.4: The ionic liquid catalyst

This IL catalyst is stated to be used due to its "operational simplicity, water-resistance, low cost [...], high yields" and "applicability to large-scale reactions..." [27]. After the reaction, liquid extraction is used to separate the nitrile compound from the reactants and catalyst, using ethyl acetate as the extraction liquid [27]. A paper by Sun et al. describes the formation of the same nitrile compound, from the same reactants. The same reaction conditions were used as well, although with an even more complex IL catalyst [28].

Further, the hydrogenation of a nitrile compound is rather complex due to the formation of highly reactive intermediates. In a patent by Fruth el al. from 1992 [29], the hydrogenation of unsaturated fatty acid nitriles is described. In this process, a fatty acid nitrile is hydrogenated over a Raney nickel catalyst during 7 hours in a stirred autoclave to produce a primary amine [29]. An addition of liquid ammonia is presented before the injection of

hydrogen (1.5 mol ammonia per mol nitrile), and the hydrogenation process results in a 97% yield of the primary amine, along with a diamine and a triamine [29].

3.2 Life Cycle Assessment

Life Cycle Assessment (LCA) is a method used to assess how a product affects elements such as resource use, human health and ecological consequences during its lifetime. An assessment that takes into account every emission released from the raw material acquisition to the production and use, including the products end-of-life, is called a cradle-to-grave assessment. Although, often it is not necessary to assess the whole lifetime of the product. Instead, by excluding use and end-of-life, a cradle-to-gate assessment can be made, counting every emission from raw material acquisition until the finished product. A third option is to make a gate-to-gate assessment, only looking at the production of a product, excluding raw material acquisition, use and disposal [30].

3.2.1 Inventory Analysis

To be able to assess the impacts, an inventory analysis of relevant inputs and outputs is conducted. For that reason, a system model is constructed, producing a mass and energy balance, while considering relevant flows [30]. What is relevant to include is decided during the first part of the assessment, considering the goal of the assessment as well as what kind of LCA will be conducted. There are three ordinary types of LCA; accounting LCA, change-oriented LCA, and stand-alone LCA. The accounting LCA considers the cumulative inputs and outputs in the whole process, striving for a completeness of the assessment. A change-oriented LCA considers only those steps that are directly affected in the system, and is usually used when comparing impacts of two, or more, products. A stand-alone LCA, on the other hand, is made to describe a single product, and is the most common type of LCA used in the industry [30].

3.2.2 Life Cycle Impact Assessment

The goal of the LCA is also considered when deciding what categories, also known as midpoint indicators, to use in the Life Cycle Impact Assessment (LCIA). Categories that can be considered are for example global warming potential (GWP), cumulative energy demand (CED), land use etc. These midpoint indicators can later be weighted together into endpoint indicators. There are several different ready made methods to do the LCIA. ReCiPe is such a method, using 18 midpoint indicators and the endpoint indicators Damage to Human Health, Damage to Ecosystems, and Damage to Resource Availability [31].

In this study, the impact data for total ReCiPe (H.A), measured in points, CED, measured in MJ-equivalents, and GWP (100a), measured in kg CO_2-equivalents, was used, taken from Ecoinvent v.3.4. CED counts the net calorific value of the energy sources required

in the assessed system [32]. GWP (100a) uses a time horizon of 100 years, counting the radiative forcing induced by the emission of a greenhouse gas over a 100 years, compared with the induced radiative forcing by the same amount of emissions of CO_2 [33].

4

Methodology

The method used in the project was divided into two steps. First, the production of the studied compounds were modelled using Aspen Plus v.10. Secondly, stand-alone cradle-to-gate LCAs were performed based on the material and energy balances of the Aspen models.

4.1 Process modelling

The purpose of the modelling step was to create a process model of the production of each compound in order to get material and energy balances. As no kinetic or equilibrium values were found, key data from the patents described in Chapter 3 was used as a base to complete the simulations.

The goal of the modelling step was to get the process energy demand and the recovery in reactants, which were the keys parameters governing the results of the LCA. To that extent, two key parameters was found in the modelling step; the conversion set in the reactor (along with the presence of byproducts), and the pressure of the distillation columns, having reflux ratios as low as possible in order to minimize the energy demand (the detailed procedure for the modelling of the distillation columns are presented in Appendix A). Making different models, using different values of these key parameters, enabled a rough sensitivity analysis of the Aspen models. The key parameters changed between the models are further explained in Chapter 4.1.1-4.1.3. However, this methodology does not enable rigorous sensitivity analyses, but gives a feasible range of energy consumption and recovery of reactants for the different production processes.

Several assumptions were made for all models, the assumptions for the specific models are stated below in chapters 4.1.1-4.1.3. However, some of the assumptions were the same for all of the models. The efficiencies of the pumps and compressors used in all models are stated in Appendix B (Table B.1), these efficiencies were chosen according to usual values found in the industry. All pressure losses in the pipes of the processes were neglected due to the unknown length of pipes.

Further, the retained thermodynamic equation model for all the models was NRTL. NTRL was chosen as all the compounds were polar, non-electrolyte and with binary interaction parameters. The LLE parameters were manually provided to Aspen. In some sections

of the models, however, the pressures are higher than the NTRL limit at 10 bar. These pressures are between 1.5-3 times higher than the limit. The distillation units working under those high pressures (where the vapour-liquid equilibrium is important) all separate mostly user-defined compounds. The lack of data for those compounds make the use of the high pressure models, such as SR-polar or PRWS, impossible. Thus, the NTRL model was chosen for all models.

To check if the models would be industrially feasible, and not require unrealistic sized reactors, the reactor sizes were estimated by

$$V_{react} \approx \tau_{liq} Q_{liq} + \tau_{gas} Q_{gas} + V_{cat} + V_{safe}$$

where V_{react} was the reactor volume, τ_{liq} and τ_{gas} was the retention time of the liquid and gas respectively, Q_{liq} and Q_{gas} was the flow rate of liquid respectively gas into the reactor, V_{cat} was the catalyst volume, and V_{safe} was a safety margin. For the estimation, the added catalyst volume and safety margin was together assumed to be equal to the liquid volume ($\tau_{liq}\mathrm{Q}_{liq}$). The reactors were assumed to be industrially feasible while below 12 m^3, due to the small mass flow rate of product exiting the plant, always below 400 $\mathrm{kg.h}^{-1}$.

The recovery of the reactants were also monitored during the modelling, as mentioned above. The recovery was calculated by

$$\mathrm{rec}_i = \frac{\nu_i \mathrm{F}_P}{\nu_P \mathrm{F}_{R_i}}$$

where rec_i was the recovery of reactant i, F_P was the flow rate of the product out of the production process, F_{R_i} was the flow rate of reactant i into the reactor, and ν_P and ν_i was the stoichiometric relation between the product and the reactant in the chemical reaction $\Sigma\nu_P\mathrm{P} = \Sigma\nu_i\mathrm{R}_i$.

4.1.1 DMCA

The modelled DMCA production process is shown in figure 4.1.

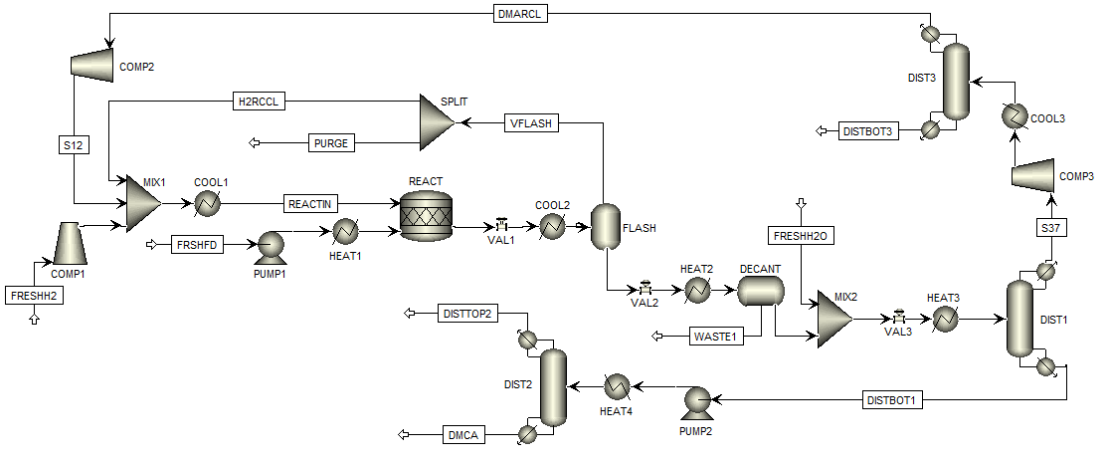

Figure 4.1: DMCA production model

The patent by Efner [22] was chosen as a base for the DMCA production model. This patent was chosen due to three main factors. First, small amounts of only one byproduct were produced during the reaction. Second, the conversion of cyclohexanone was excellent, and the yield of DMCA was also higher than 97 mol% [22]. Finally, the third deciding factor was that the reaction occured with a Raney copper catalyst, eliminating the need for rare earth metals used in the other patents.

The patent describes batch results, which were used to model a continuous process. The fresh feed consisted of a liquid mixture of 4 mass% cyclohexanone in acetic acid, and dimethylamine (DMA), with a ratio of 1.1:1 between DMA and cyclohexanone. Hydrogen was fed into the reactor at 17 bar (250 psi in the patent). To be able to assume a complete conversion of the intermediate imine compound into DMCA, as observed in the patent [22], a molar ratio of 5:1 between hydrogen and cyclohexanone was assumed, as no specific ratio or flow rate was stated in the patent.

In the model, the reactants were fed separately according to their phase (gas or liquid) into the reactor. That way the suitable compression unit, either a pump or a compressor, could be used. The reactants were then heated up to the reactor temperature 115 °C in separate heat exchangers. As no kinetic or equilibrium data were available for the reactions, a stoichiometric reactor was used in the model. The chemical equations (4A) and (4B) were entered, with the cyclohexanone conversions of 0.96 and 0.005 respectively.

$$\begin{aligned} \text{Cyclohexanone} + \text{DMA} + \text{H}_2 &\longrightarrow \text{DMCA} + \text{H}_2\text{O} \quad (4A) \\ \text{Cyclohexanone} + \text{H}_2 &\longrightarrow \text{Cyclohexanol} \quad (4B) \end{aligned}$$

At the reactor outlet, the crude mixture was cooled to 5°C, in order to separate the hydrogen from the other compounds in a flash. The hydrogen was then recycled back into the reactor. A purge stream was added to prevent the accumulation of other compounds,

such as cyclohexanol. A second recycling loop from the separation part sent the unreacted DMA back to the reactor.

The separation process described in the patent was a lab-scale process, that, in the case of scaling it to the industrial level, would require a large amount of energy. Therefore, the modelled process did not follow the described separation. In order to reduce the energy demand, a decanter was added, to get rid of the aqueous phase containing some impurities. The NRTL binary parameters for the LLE were not available in Aspen Plus. As the mixture consisted mainly of DMCA and water, experimental data from the ROLINCAP project [9] was used along with the regression tool of Aspen Plus in order to get the parameters presented in Table 4.1.

Table 4.1: DMCA(i)/Water(j) NRTL binary parameters

	ij	ji
A	12.2765	2.24237
B	-3884.57	1236.06
C	0.3	-

After the decanter separation, fresh water was added as a solvent to get rid of the impurities in the high-boiling phase. Water was chosen as a solvent due to its low price, non-toxicity and availability. During the modelling, it was proven that a large amount of water in the column enabled a better purification of DMCA at the condensate. The distillation separation was chosen after it was proven to result in a more pure product than two decanters could give. It is possible that more than two decanters in series could result in the same purity as the distillation column, although with higher DMCA losses, however, this was not examined further.

In order to reduce the energy consumption, the distillation (DIST1) was operated under vacuum (0.02 atm). This way, the condensate from the first column reaches a temperature of 14.77°C. Due to an assumption that cooling water could be used to cool down to 15°C, the distillation therefore avoids the use of brine.

Due to the low pressure in the first column, a second (atmospheric) column (DIST2) was added to purify the DMCA up to 99 mol% from the bottom product of the first column. A second solution was explored, using a pressure of 0.01 atm in the first column. That way there was no need of a second column and the DMCA losses in the distillate were lowered, since the lowered pressure induced a better separation between water and DMCA. However, it required an extremely high brine flow rate (about 27 000 $kg.h^{-1}$) for the distillate, making it industrially unfeasible.

A third column (DIST3) was added to recover and recycle the unreacted DMA from the distillate of the first column. That distillation was done under atmospheric pressure, to reduce the cost of the unit, which was feasible since the boiling point of the light compounds (ammonia and DMA) were very low. The boiling point of the distillate was low enough to not have to go to lower than atmospheric pressure, but not low enough to require a higher pressure than atmospheric.

The impact the reflux ratio in the distillation columns had on the process energy demand was explored further. The reflux ratio in the columns was changed between 30 and 50, and plotted against the heat demand of the process, the results are shown in Chapter 5.1.1.

The main parameters set during the modelling described above are presented in Table 4.2, it is also presented whether the parameter was set according to a source, estimated based on a source, or assumed due to a lack of data.

Table 4.2: Main parameters set during the DMCA production modelling

	Set according to	Estimated based on	Assumed
Continuous process		[22]	
1.1:1 ratio of DMA:cyclohexanone	[22]		
5:1 ratio of H_2:cyclohexanone			X
Reactor temperature 115°C	[22]		
Cooling to 5°C (COOL2)			X
NRTL binary parameters		[9]	
Water as separation solvent			X
Vacuum distillation (DIST1)			X
Atmospheric distillation (DIST2)			X
Atmospheric distillation (DIST3)			X
Reflux ratio (DIST1/2/3)			X

4.1.2 MCA

The modelled MCA production process is shown in Figure 4.2.

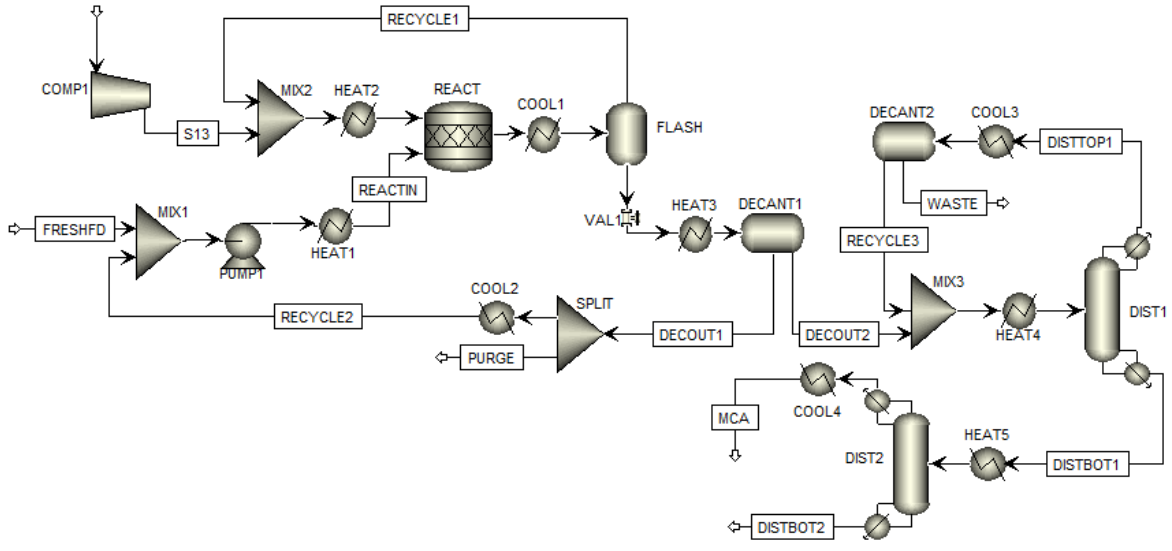

Figure 4.2: MCA production model

The model for MCA was developed using mainly the two Chinese patents presented in chapter 3.1.2. The production of MCA follows a similar procedure as for the production of DMCA. The major difference lies in the reaction conditions, as the MCA reaction occurs under aqueous conditions. Methylamine was introduced as a 27 mass% aqueous solution together with 98 mass% pure cyclohexanone. The reaction occured under 3.5 bar pressure and the components in the feed were compressed and preheated separately according to their state (vapor or liquid). It was described that the reactor temperature was maintained at 150 °C due to a cooling system.

Due to the patents not stating anything about byproducts, two different models were made. MCA_1 was made using the assumption that byproducts would be produced in the same way as for DMCA, while assuming that the process would convert the same amount of reactant as in the patent. This assumption led to a yield of 96 mol% MCA, and a 2 mol% yield of the byproduct cyclohexanol was assumed. As no acetic acid was used in the MCA production, there might be other possible byproducts, however those were not investigated further. MCA_2 refers to a model assuming that no byproducts would be produced, with the yield assumed to be 98% as stated in the patent.

The modelled separation did not follow the separation described in the patent. Instead, the separation used two distillation columns and the liquid-liquid equilibrium properties of the MCA/water mixture through the use of two decanters. Once again, the LLE parameters were not present in the database of Aspen Plus. The NRTL binary parameters were therefore estimated using ROLINCAP equilibrium data and the regression tool of Aspen Plus (values presented in Table 4.3).

Table 4.3: MCA(i)/Water(j) NRTL binary parameters

	ij	ji
A	8.45219	-0.429416
B	-3273.97	2245.77
C	0.3	-

While making sure that the dimension of the units in the model were not infeasible, the MCA was purified according to the following two steps; (1) the outlet of the reactor was cooled down to 5°C, preserving the pressure of the reaction section of 3.5 bar, and recycling the hydrogen using a flash. (2) The liquid mixture was expanded up to 1 atm and heated up to 98 °C before being sent to a decanter. The LLE parameters in Table 4.3 corresponded to that pressure, and that pressure was subsequently chosen as it offered the best certainty, even though the liquids were assumed to be non-compressible. The mixture was heated as much as possible, to barely below the VLLE equilibrium, the triphasic line, since those conditions provided the best possible separation between MCA and water, i.e. the separation provides the best split without formation of a gas phase.

The organic phase was then sent to a first distillation column (DIST1; MCA_1 and MCA_2 using atmospheric distillation). Due to the difficult separation, a significant fraction of MCA was lost in the distillate, along with water, because of the liquid-liquid-vapor equilibrium. To avoid losing it definitely, the distillate was sent to a second decanter operating under similar conditions as the first one. That way an additional amount of

water was eliminated without the high energy requirements of a distillation column. The organic phase of the second decanter, containing mainly MCA, was then recycled to the feed of the first column.

A final distillation column (DIST2) was added after the condensate of the first one to further purify the MCA, reaching at least 99 mol% purity at the end of the process. It was observed that operating DIST2 under vacuum decreased the energy requirement of the column.

It was tested to purify the distillate from DIST1 by sending it directly to the second distillation column. However, as the distillate contained only 63 mol% MCA, it resulted in a significantly lowered purity of the product at the end of the process. The recycling of the distillate implemented in the models resulted in a high flow rate at the feed of the first column, increasing the energy demand. However, it enabled a high recovery of the reactants and a high purity of the product.

Trying to decrease the energy demand of the models, two additional models were made, using a pressurized distillation. MCA_3, using the same yield and byproducts as for MCA_1, and MCA_4, using the same yield and byproducts ad for MCA_2. The pressures used was determined as described in Appendix A.

The main parameters set during the modelling described above are presented in Table 4.4, whether the parameter was set according to a source, estimated based on a source, or assumed due to a lack of data is also presented.

Table 4.4: Main parameters set during the MCA production modelling

	Set according to	Estimated based on	Assumed
Continuous process		[25]	
27 mass% aq. methylamine	[25]		
98 mass% cyclohexanone	[25]		
Reaction pressure 3.5 bar	[25]		
Reactor temperature 150°C	[25]		
Byproduct		[22]*	X*
Yield	[25]*	[25]*	
NRTL binary parameters		[9]	
Cooled to 5°C (COOL1)			X
Expansion to 1 atm (VAL1)			X
Heating to 98°C (HEAT3)			X
Vacuum distillation (DIST2)			X

* *see Table 4.5*

Table 4.5 present the different assumptions in the different models.

Table 4.5: Assumptions made in the different models for the production of MCA

	MCA_1	MCA_2	MCA_3	MCA_4
96% yield	X		X	
98% yield [25]		X		X
Byproducts	X		X	
No byproducts		X		X
Atmospheric distillation	X	X		
Pressurized distillation			X	X

4.1.3 MAPA

The modelled MAPA production process is shown in Figure 4.3. The modelling of the MAPA production was based on the paper by Jiang et al. described in chapter 3.1.3, as well as the patent by Fruth et al. described in the same chapter. Although the paper and patent describes laboratory-scale reactions, the results were used as a base in the large-scale production modelled. Two separate stoichiometric reactors were used to model the reactors for the two separate reactions. Because of the uncertainties on the actual production process, several models were made.

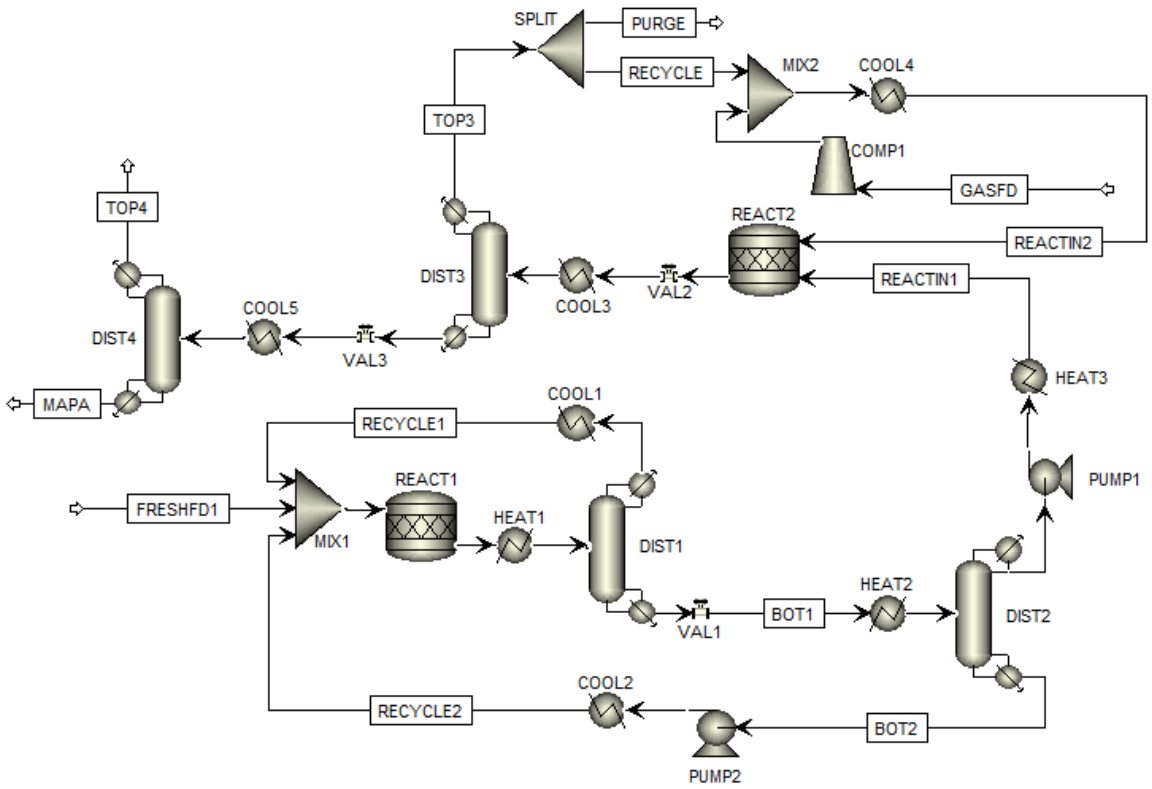

Figure 4.3: MAPA production model

In the first model ($MAPA_1$), it was assumed that in the first reactor (REACT1), the conjugate addition of acrylonitrile and methylamine would have a 80% yield. This was assumed due to the likelihood that the yield would decrease in the scaling of the process from laboratory- to large-scale production. This assumption was removed in the second model ($MAPA_2$), where the yield was assumed to be 99% as in the paper. These assumptions were the only difference between $MAPA_1$ and $MAPA_2$.

Due to difficulties of adding an ion as a compound into Aspen Plus, the IL catalyst was modelled as a non-charged compound. Several different compounds were considered, although in the end, 5-oxo-5-(pyridyl)valeric acid (OVA) (figure 4.4) was used.

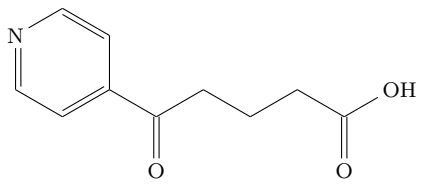

Figure 4.4: 5-oxo-5-(pyridyl)valeric acid (OVA)

There were three main reasons for using OVA to model the IL catalyst; structural similarity to the IL catalyst, boiling point and heat capacity. An IL has an extremely high boiling point, or has no boiling point at all, and OVA had an atmospheric boiling point of 434^oC. This was about 160°C above the highest estimated boiling point out of the other compounds used in the model. Further, OVA has an estimated heat capacity of 0.843 $kJ.kg^{-1}.K^{-1}$ according to the Aspen estimation. A paper from J.S. Wilkes states that the heat capacity for some common ionic liquids range between 1.196-1.659 $kJ.kg^{-1}.K^{-1}$ [34]. As the IL catalyst mass fraction in the models were only about 1.2 mass%, the heat capacity of OVA was considered to be close enough in order to model the catalyst with reasonable results.

In the models, the separation of the product from reactants and catalyst was done by liquid extraction in both $MAPA_1$ and $MAPA_2$, as stated in the paper. A separator block was used to model the liquid extraction (not included in Figure 4.3). The extraction liquid ethyl acetate was added after the reactor right into the separator together with the reactor outlet stream. It was assumed that 100% of the IL catalyst could be separated and recycled. Jiang et al. specified that 2×20 mL of ethyl acetate was used for 20 mmol of introduced methylamine [27], and the same ratio was kept in the model. As a perfect separation was assumed, the separation block was assumed to model the two extraction columns in series that would exist in reality.

However, is was discovered that the boiling points of the extraction liquid (ethyl acetate) and acrylonitrile only differed about 0.1°C at atmospheric pressure. This made it impossible to separate them in a feasible way for industrial use, making them impossible to recycle. Therefore, in $MAPA_1$ and $MAPA_2$, ethyl acetate and acrylonitrile was not recovered or recycled, and sent to a hypothetical waste treatment plant. Liquid extraction were therefore deemed infeasible for industrial use, and it was decided to make further models using distillation as a separation method instead of the liquid extraction. Due to time restraints, a simplified hydrogenation were used to complete $MAPA_1$ and $MAPA_2$, assuming a yield of 100% and that no ammonia would be present in the reaction.

Two additional models were made ($MAPA_3$ and $MAPA_4$). These models used the same yield assumptions and the same simplified hydrogenation assumptions, as for $MAPA_1$ and $MAPA_2$, but with distillation separation (shown in Figure 4.2). $MAPA_3$ and $MAPA_4$ showed that without the use of an extraction liquid the unreacted reactants could be recycled, reducing the demand of new reactants, as well as cancelling the demand of the extraction liquid itself. The first distillation column (DIST1), used to separate unreacted reactants, operated under atmospheric pressure. The second column (DIST2), separating the IL catalyst, used a reduced pressure (0.1 atm). The boiling point of the intermediate nitrile compound formed in the first reactor was very high and the reduced pressure reduced the energy demand of the separation unit. However, no estimation of the energetic cost of the production of lower pressure was made.

The distillation separation was considered to be industrially feasible. Therefore, models $MAPA_5$ and $MAPA_6$ were made, expanding the hydrogenation part of the models using distillation separation. $MAPA_5$ was made using the same basic assumptions as for $MAPA_3$, and $MAPA_6$ with the same assumptions as for $MAPA_4$. Into the second reactor, ammonia and hydrogen was introduced. The ammonia was kept at a 1.5:1 molar ratio (1.5 mol ammonia to 1 mol nitrile compound) [29]. Gaseous ammonia was used in the models, even though it was stated to be liquid in the paper. This had to be done due to difficulties of using liquid ammonia in Aspen Plus. The hydrogen inlet was set with an arbitrarily chosen molar ratio of 4:1 (hydrogen to nitrile compound), assumed to give a big enough excess of hydrogen for the hydrogenation to take place.

The separation after the hydrogenation required two distillation columns. The first column (DIST3) separated hydrogen and ammonia from the product stream. A distillation column was used since a flash proved not to be efficient enough. To eliminate the demand for brine in the process, the pressure in the first distillation column was adjusted to 17 bar in $MAPA_5$ and 18 bar in $MAPA_6$. However, this decision resulted in an increased demand for natural gas-powered fire heating instead. A purge was added to the gas recycling loop, to avoid the accumulation of ammonia in the loop. The second distillation column (DIST4) was set to work under a reduced pressure (0.1 atm), to purify the MAPA.

Table 4.6 states the main assumptions made in the different models of the production of MAPA.

Table 4.6: Assumptions made in the different models for the production of MAPA

	$MAPA_1$	$MAPA_2$	$MAPA_3$	$MAPA_4$	$MAPA_5$	$MAPA_6$
80% yield	X		X		X	
99% yield [27]		X		X		X
Liquid extraction [27]	X	X				
Distillation			X	X	X	X
Ideal hydrogenation	X	X	X	X		
Real hydrogenation [29]					X	X

The main parameters set during the modelling described above are presented in Table 4.7, whether the parameter was set according to a source, estimated based on a source, or assumed due to a lack of data is also presented.

Table 4.7: Main parameters set during the MAPA production modelling

	Set according to	Estimated based on	Assumed
Continuous process		[27, 29]	
Yield	[27]*		X*
Catalyst OVA		[27]	
Liquid extraction	[27]*		
Distillation separation			X*
IL catalyst recycling 100%			X
Ratio IL catalyst:methylamine	[27]		
IL catalyst separation 100%			X
1.5:1 ratio of NH_3:nitrile	[29]		
Gaseous NH_3		[29]	
4:1 ratio of H_2:nitrile			X
Pressurized distillation (DIST3)			X
Vacuum distillation (DIST4)			X

* *see Table 4.6*

4.2 Life Cycle Assessment

4.2.1 Goal and Scope

The functional unit used in the assessment was *1 kg of produced product*, where the product consisted of either DMCA, MCA or MAPA. The impact categories used were GWP(100a) and non-renewable CED, as well as the characterization model total ReCiPe (H,A).

4.2.2 Inventory analysis and Impact Assessment

For all modelled processes, the cradle-to-gate boundaries used for the LCA is shown in figure 4.5. All extracted data from the models used in the LCA are presented in Appendix C. The data used for raw material acquisition and chemical production was cradle-to-gate LCA results for the specific process chemicals from Ecoinvent v.3.4, and are presented in Appendix C, table C.1.

However, due to the unspecified exact locations of the modelled processes, the impact from the transportation between the process chemical production and the modelled plants were not included in the LCA. In the same way, any potential transportation of waste or wastewater to treatment or incineration plants was excluded.

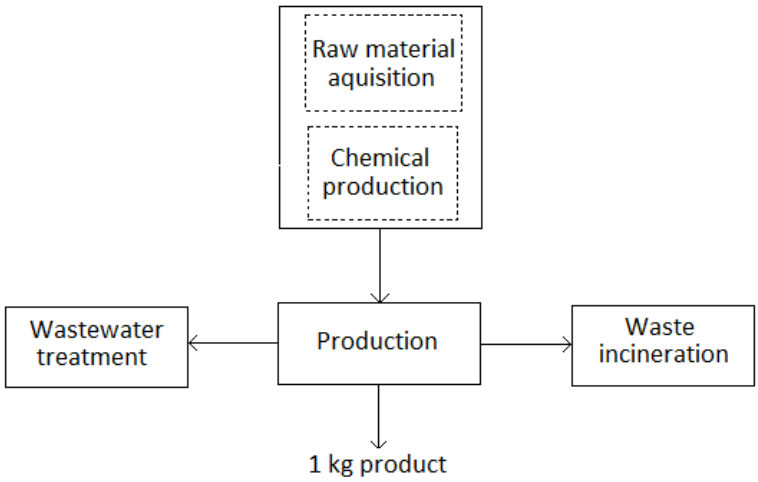

Figure 4.5: Cradle-to-gate boundaries

It was assumed that the electricity demand was covered by an European electricity mix, due to the assumption that all modelled productions are placed in Europe. All cooling above 15^{o}C was assumed to be covered by cooling water from a nearby lake or sea. The impact from the use of the cooling water was considered negligible. Cooling below 15^{o}C was assumed to be covered by brine. The heating demand below 250^{o}C was assumed to be covered by steam from European chemical industries, and all heating above that was assumed to be covered by natural gas-powered fire heating. The impact data used in the LCA calculations for the utilities and electricity were taken from EcoInvent v.3.4 and are presented in Appendix C, table C.1.

To estimate the utility consumption in the models, a 10°C ΔT_{min} was assumed in all heat exchangers, corresponding to the default value of the Aspen Energy Analyzer. The brine was assumed to be an aqueous solution with 22.64% NaCl, corresponding to a heat capacty of 3.315 kJ.kg^{-1}.K^{-1} [35]. The NaCl content was chosen to correspond to a liquefaction temperature at -20°C. For safety reasons, the minimum temperature available for the brine $T_{brine,min}$) was assumed to be -19°C. The brine demand flow rate was subsequently calculated as

$$\dot{m}_{brine} = \frac{Q_C}{Cp_{brine} * |(T_{H,min} - \Delta T_{min}) - T_{min,brine}|}$$

where the $\dot{m}_{brine}$ was the brine flow rate in kg.h^{-1}, the Q_C was the cooling demand below 15°C in kJ.h^{-1}, Cp_{brine} was the brine heat capacity in kJ.kg^{-1}.K^{-1}, $T_{H,min}$ was the hot stream outlet temperature in K, and $T_{brine,min}$ was the brine inlet temperature in K.

Because all the heating demand above 250^{o}C stems from the reboilers, and the reboilers were assumed to be one unit using one type of heating medium, the natural gas demand flow rate was calculated as

$$\dot{m}_{gas} = \frac{Q_H}{\Delta H_c}$$

where $\dot{m}_{gas}$ was the natural gas flow rate in kg.h^{-1}, Q_H was the heating demand above 250°C in MJ.h^{-1} and ΔH_c was the average gross heating value of natural gas (48.8481 MJ.kg^{-1} at 15.6°C and 1 atm [36]).

The steam demand used in the LCA calculations was the total heating demand from the heat exchanger network, manually compiled by the Aspen Energy Analyzer. In the models requiring fire-heating, the duties from the fire-heating streams were subtracted from the total heating demand, while assuming the rest would be covered by steam.

Further, the impact from waste incineration, as well as for the wastewater treatment (WWT), was estimated by using waste treatment models [37]. The waste streams containing high amounts of hydrogen were also assumed to be incinerated. This incineration were first assumed to be located at the production plant, using the heat generated to heat the process. However, due to a very slight amount of hydrogen waste in each process, it was deemed unrealistic, and the stream was instead assumed to be incinerated in a hypothetical central waste treatment plant. All waste stream compositions for all models are presented in Appendix C, table C.3, and all estimated impacts are presented in table C.2.

All processes modelled requires the use of catalysts. To be able to estimate the amount of make-up of catalyst needed during a continuous production, a few assumptions were made; (1) the solid catalysts would be used for 500 hours before replacement in a continuous industrial reaction, (2) the IL catalyst would be used for 100 hours before replacement, and (3) the reaction conditions would be identical to the conditions described in the patents or articles. The required flow rates of catalysts were consequently calculated as

$$\dot{m}_{cat} = \frac{\frac{N_{cat}}{N_{reactant}} * t_{reaction} * \dot{m}_{reactant}}{t_{cat}}$$

where $\dot{m}_{cat}$ was the catalyst flow rate in kg.$^{-1}$h (or mol.$^{-1}$h), N_{cat} was the amount of catalyst used in mol (or kg), $N_{reactant}$ was the amount of reactant used in mol (or kg), $t_{reaction}$ was the reaction time in hours, $\dot{m}_{reactant}$ was the mass flow of reactant into the reactor (extracted from the model) in kg.h^{-1} (or mol.h^{-1}), and t_{cat} was the assumed time the catalyst would be used before being replaced (in hours). Everything but $\dot{m}_{reactant}$ and t_{cat} was found in the patent or paper. The catalyst make-up flow rates are presented in Appendix C, table C.4.

All impacts assessed during this project was also estimated using a short-cut FineChem model [38]. The model allows an estimation of the impact of the manufacturing of the molecule based on its composition and structure. FineChem claims to have an error margin of 40%, and this range was compared to the impacts assessed during this project (see chapter 5.2).

4.2.2.1 DMCA

The utility demands and flow rates of needed chemicals were extracted from the Aspen model of the DMCA production. The flows were recalculated as demand per kg of produced DMCA, based on the production flow. The demands are presented in Appendix B, Table B.5, and the production flow rate in Table B.2.

The modelled production process of DMCA requires the use of a Raney copper catalyst. According to the patent, 0.02 kg of catalyst was used to react 10 mol of DMA in a batch reactor during 2 hours [22]. The molar flow of DMA into the reactor was extracted from the Aspen model (109 $kmol.h^{-1}$). The make-up flow of catalyst required were then calculated as described in Chapter 4.2.2.

The environmental impact from the production of the make-up catalyst needed in the process were assumed to be identical to the impact of the global production of copper. The transportation of the copper to the DMCA production cite was excluded.

4.2.2.2 MCA

The utility demands and flow rates of needed chemicals were extracted from the Aspen models of the MCA production, both for the models including and excluding byproducts. The flows were recalculated as demand per kg of produced MCA, based on the production flows extracted from the models. The demands are presented in Appendix B, Table B.5, and the production flow rate is presented in Table B.2.

As described in chapter 3.1.2, the production of MCA is supported by a palladium-on-carbon catalyst. However, the patent does not state the amount of catalyst used in the production. Therefore, it was assumed that the catalyst make-up flow rate would be an average of the metallic catalyst make-up flow rates calculated for the other productions modelled in the project. The subsequent flow rate of palladium and carbon needed for the LCA calculations were then calculated by assuming a 10 wt.% palladium composition of the catalyst [39].

4.2.2.3 MAPA

The utility demands and flow rates of needed chemicals were extracted from the Aspen models of the MAPA production. The flows were recalculated as demand per kg of produced MAPA, based on the production flows extracted from the models. The demands are presented in Appendix B, Table B.5, and the production flow rate in Table B.2.

As described in chapter 3, the production of MAPA requires two different catalysts. The article describing the use of the IL catalyst states the use of 0.14 mmol catalyst to react 0.02 mol CA for 5 minutes in a batch reactor [27]. The molar mass of the IL was calculated to 330.82 $g.mol^{-1}$ and the molar flowrate of methylamine into the reactor was extracted from the Aspen model. The flow rates of the IL catalyst were calculated in accordance to the method described in chapter 4.2.2.

The environmental impact of the IL catalyst was thereafter assumed to be the impact from 50 mol% iron sulfate and 50 mol% organic compound (shown in Figure 3.4, Chapter 3). The impact from the organic compound was estimated using the FineChem estimation tool.

Also, the hydrogenation requires a metallic catalyst. The patent used as a base for the hydrogenation part of the model describes the hydrogenation of 3.5 mol of nitrile over 30 g of Raney nickel catalyst with a reaction time of 3.5 hours [29]. The nitrile molar flow rate into the hydrogenation reactor was extracted from the Aspen models. The flow rates of the nickel catalyst were calculated according to the method described in chapter 4.2.2.

5

Results and Discussion

5.1 Process modelling

The energy and chemical utilities demand from all models are presented in Appendix B. The recovery of the chemicals in all models are presented in the same Appendix. Chapter 5.1.1-5.1.2 below presents the results for the models deemed to be the most realistic; DMCA, MCA_3 and $MAPA_5$.

5.1.1 DMCA

The resulting inflow demands from the DMCA model are presented in Table 5.1. The same table presents the chemical recovery, calculated as described in Chapter 4.2.2. The highest chemical demand per produced kg DMCA was from cyclohexanone, and the lowest hydrogen. This corresponds to the waste stream composition (see Appendix C, Table C.3), where the cyclohexanone content was the highest out of the reactants. Also, it was observed (as presented in Table 5.1), that out of the reactants, cyclohexanone had the lowest recovery.

Table 5.1: DMCA model demands per kg DMCA and recovery results, based on a production of 120.81 $kg.h^{-1}$ DMCA

	[*]	Demand [$*.kg^{-1}_{DMCA}$]		Demand [$kg.kg^{-1}_{DMCA}$]	Recovery [mol%]
Electricity	[kWh]	0.0878	Acetic acid	0.0325	-
Steam	[MJ]	15.415	Cyclohexanone	0.8124	94.02
Brine	[kg]	1.1679	Dimethylamine	0.3655	96.00
			Hydrogen	0.0161	97.31
			Water	0.0552	-

The estimated reactor size and distillation column slenderness ratio are presented in Table 5.2. It was observed that distillation column DIST3 (purifying dimethylamine before recycling), resulted in a higher distillation ratio than the upper limit of 20. To answer to the standard sizes of industry, this column therefore would need to be more rigorously

sized. However, the rest of the columns fit comfortably in the distillation ratio range between 3 and 20, and the reactor size of 1.2 m^3 was deemed industrially feasible.

Table 5.2: Estimated reactor size and distillation ratios for DMCA

Reactor [m^3]	DIST1 [ø]	DIST2 [ø]	DIST3 [ø]
1.2	6.7	20	25

Figure 5.1 shows the results from the sensitivity analysis of the reflux ratio on the process energy demand. As can be observed, DIST1 governs the heat demand, because it has the biggest reboiler duty. A reflux ratio of 35 and 40 were first used in the model, for DIST1 and DIST2 respectively. However, the energy demand could be lowered further by lowering the reflux ratio of DIST1 to 30, and a linear relationship between the reflux ratio and the energy demand was observed. The reflux ratio of DIST2, as well as DIST3 (not plotted in Figure 5.1), was observed to have close to no impact on the process energy demand, in comparison to the impact of DIST1.

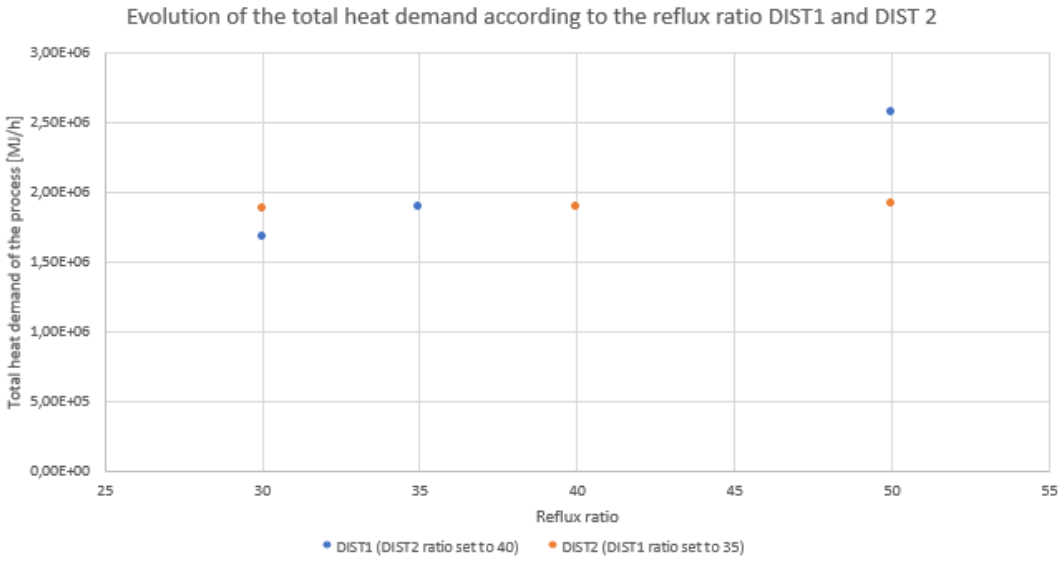

Figure 5.1: Total heat demand changing with different reflux ratios

Since no cost estimations were made during this project all the models of the project have reflux ratios set as low as possible. That was done in order to minimize the energy demand. A range of the total process energy demand for the production of DMCA for different reflux ratios in column DIST1 are presented in Table 5.3.

Table 5.3: Total energy demand and product flow, depending on reflux ratio in DIST1

Reflux ratio	Total Energy demand [$MJ.h^{-1}$]	Product flow rate [$kg.h^{-1}$]
30	1684.80	119.35
35	1862.23	120.81
50	2575.76	119.63

5.1.2 MCA

The resulting inflow demands from MCA_3 are presented in table 5.4. The same table presents the chemical recovery, calculated as described in Chapter 4.2.2. The highest chemical inlet flow rate was cyclohexanone, and the lowest hydrogen.

Table 5.4: MCA_3 demand and recovery results per kg MCA, based on the production of 380.91 $kg.h^{-1}$ MCA

	[*]	Demand [$*.kg^{-1}_{MCA}$]		Demand [$kg.kg^{-1}_{MCA}$]	Recovery [mol%]
Electricity	[kWh]	0.0125	Cyclohexanone	0.9005	95.5
Steam	[MJ]	11.1421	Hydrogen	0.0184	96.1
Brine	[kg]	3.4178	Methylamine	0.2757	98.7
			Water	0.0830	-

The estimated reactor size and distillation column slenderness ratios are presented in table 5.5. Both distillation ratios fit into the distillation ratio range 3-20. However, the reactor size was estimated as the upper limit of 12 m^3. A lower safety volume of 4 m^3 was therefore assumed in this case.

Table 5.5: Estimated reactor size and distillation ratios for MCA_3

Reactor [m^3]	DIST1 [ø]	DIST2 [ø]
12	9.0	6

5.1.3 MAPA

The resulting inflow demands from $MAPA_5$ are presented in table 5.6. The same table presents the chemical recovery, calculated as described in Chapter 4.2.2. The highest chemical demand per kg produced MAPA was acrylonitrile, followed by methylamine, and the lowest demand was ammonia.

Table 5.6: $MAPA_5$ demand and recovery results per kg MAPA, base on the production of 69.31 $kg.h^{-1}$ MAPA

	[*]	Demand [$*.kg^{-1}_{MAPA}$]		Demand [$kg.kg^{-1}_{MAPA}$]	Recovery [mol%]
Electricity	[kWh]	0.1239	Acrylonitrile	0.6124	96.3
Steam	[MJ]	14.8257	Ammonia	0.0027	-
Natural gas	[MJ]	0.3553	Methylamine	0.3584	96.3
			Hydrogen	0.0475	94.4

The estimated reactor sizes and distillation column slenderness ratios are presented in table 5.7. The reactors were deemed industrially feasible, with the sizes of 0.2 m^3 and 2 m^3 respectively. The distillation ratios for two columns were below 3, and assumed to be divided into several parallel columns in the industry. The remaining three columns all fit into the accepted distillation ratio range.

Table 5.7: Estimated reactor sizes and distillation ratios for $MAPA_5$

React1 [m^3]	React2 [m^3]	DIST1 [ø]	DIST2 [ø]	DIST3 [ø]	DIST4 [ø]
0.2	2	12	2	6	19

5.1.4 General discussion

Several improvements can be suggested to increase the modelling accuracy; (i) adding a compression train instead of one compressor, (ii) rigorously column sizing, and (iii) heat recovery scenarios including temperature and pressure modifications in the downstream separation section, which is currently really low for all the models. That is to say, the energy consumption could potentially be decreased. This is especially true in the MAPA models, which require very expensive fire heating. Again no cost analysis has been performed, but the use of such a utility could make the process non-profitable. It should also be pointed out, that the products are CO_2 extraction solvents, that might not be sold at a very high price, which rends even more difficult the profitability of its manufacturing process.

5.2 LCA

The cradle-to-gate LCA metrics for the production of the molecules in interest in this study (plus MEA as a reference molecule for CO_2 capture) as estimated by FineChem [38] are presented in table 5.8.

Table 5.8: Estimated impact data from FineChem

	ReCiPe (H.A) [$pt.kg^{-1}$]	CED [$MJ.kg^{-1}$]	GWP (100a) [$kg_{CO_2,eq}.kg^{-1}$]
DMCA	0.39	94.46	3.29
S1N	0.94	165.7	5.38
MCA	0.38	94.37	3.19
MAPA	0.85	141.13	4.76
MEA	0.263	105.49	3.48

The estimated impacts imply that S1N gives the highest impact in all three categories. MEA seemed to give the lowest ReCiPe impact, while MCA is lowest for both the CED and

GWP impact. FineChem estimates the impact based on the structure of the molecule. Therefore, S1N had the biggest estimated impact due to the molecule being the most complicated (S1N is presented in the confidential Appendix D). In the same way, MEA and MCA had the lowest estimated impacts due to the molecules being the least complicated. Considering DMCA and MCA, their estimated impacts are very similar in all three categories. Again, this is due to their very similar structures.

The following chapters presents the results from the LCA based on the process models. The calculated ReCiPe, CED and GWP impacts per kg of product for all models are presented in Appendix C (Chapter C.2).

5.2.1 DMCA

The cradle-to-gate LCA metrics based on the mass and energy balances from the DMCA production model are shown in Figure 5.2; Figure a) shows the ReCiPe results, Figure b) the CED results and Figure c) shows the GWP results.

The results show that the biggest impact in all three categories comes from the cyclohexanone. For ReCiPe, the second biggest impact comes from the steam, and a very close third is the dimethylamine. A similar trend can be observed for GWP, although with a slightly bigger difference in impact. However, for the CED, the dimethylamine impact comes in second, before the steam. The WWT, electricity-, hydrogen- and water demand in the model results in almost no impacts at all. The copper catalyst make-up (titled Copper in Figure 5.2) also resulted in a very small impact for both CED and GWP, however, although still small, for ReCiPe, the catalyst make-up has the fifth biggest impact.

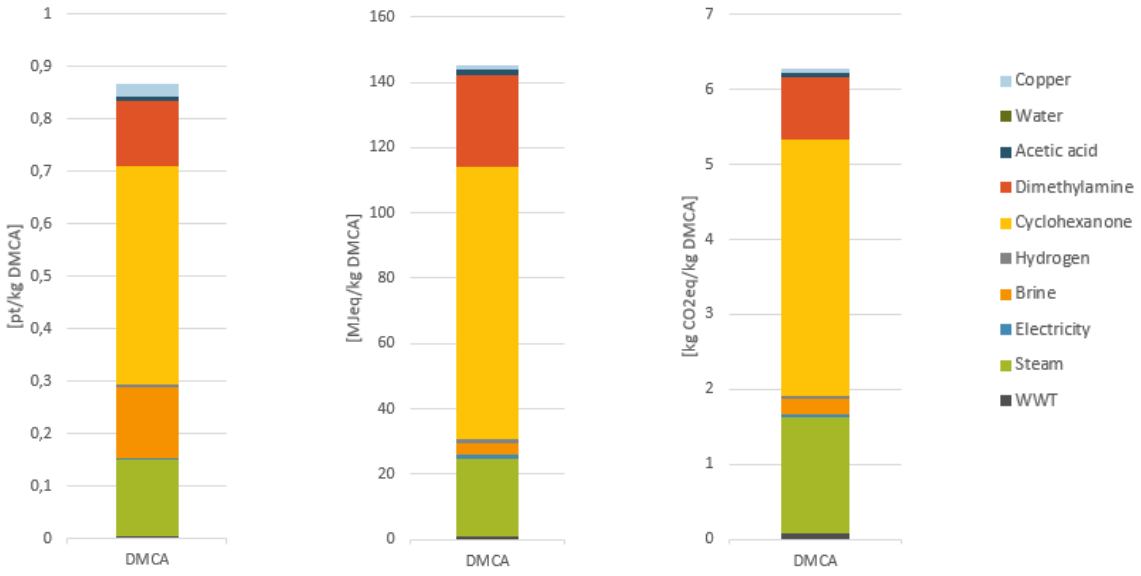

(a) ReCiPe **(b)** CED **(c)** GWP

Figure 5.2: LCA results for DMCA

Roughly estimated, the chemical demand covers between about 70-80% of the impact

in all categories. Out of that a vast majority of the impact comes from the reactants. With the model having a recovery of about 95 mol% of the reactants, it would be hard to decrease their impact further.

The impacts that are the most dependent on the model set up are the impacts from steam and brine. As the modelling have shown, different pressures and temperatures in certain components results in very different energy demands. However, due to the steam and brine only making up 20-30% of the impact, a slight decrease would not result in a big difference. This could be investigated further by modelling other production methods and/or using other pressures and temperatures. The details of the energy demand in the model was not investigated further.

The obtained range of the LCA metrics based on the senstivity analysis made on the reflux ratio in the DMCA process model are compared to the impact from the FineChem estimation tool in Figure 5.3.

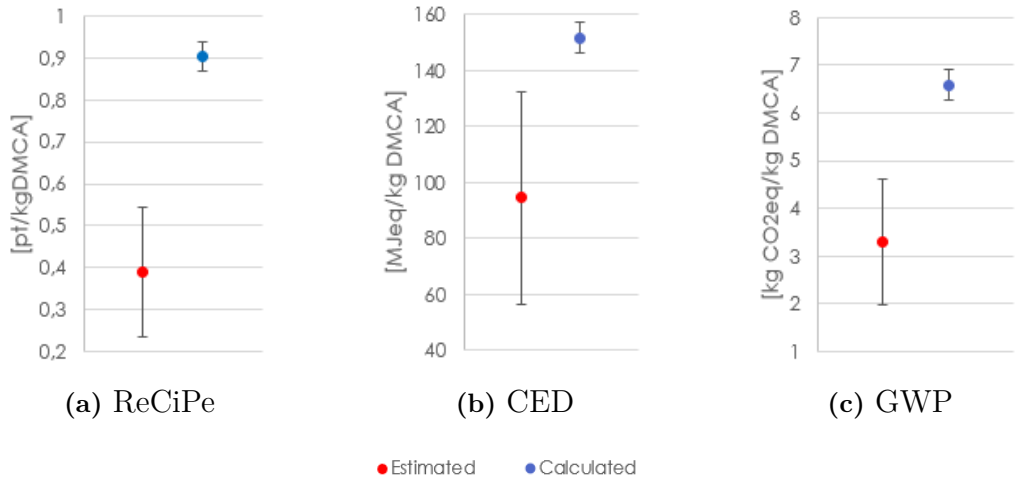

(a) ReCiPe **(b)** CED **(c)** GWP

Figure 5.3: Comparing calculated impacts to estimated impacts for DMCA

The comparison shows that all calculated impacts are higher than the FineChem estimated impacts. The differences could be due to the FineChem estimation model only considering the structure of the model, and not taking into account the actual impact from different reactants. Also, the differences could depend on that FineChem was partially based on data from Ecoinvent v.2.2, as well as the fact that the process model could be further optimized regarding the energy consumption.

5.2.2 MCA

The ReCiPe results from the LCA based on all MCA models are shown in figure 5.4 a), the CED results in b), and the GWP results in c).

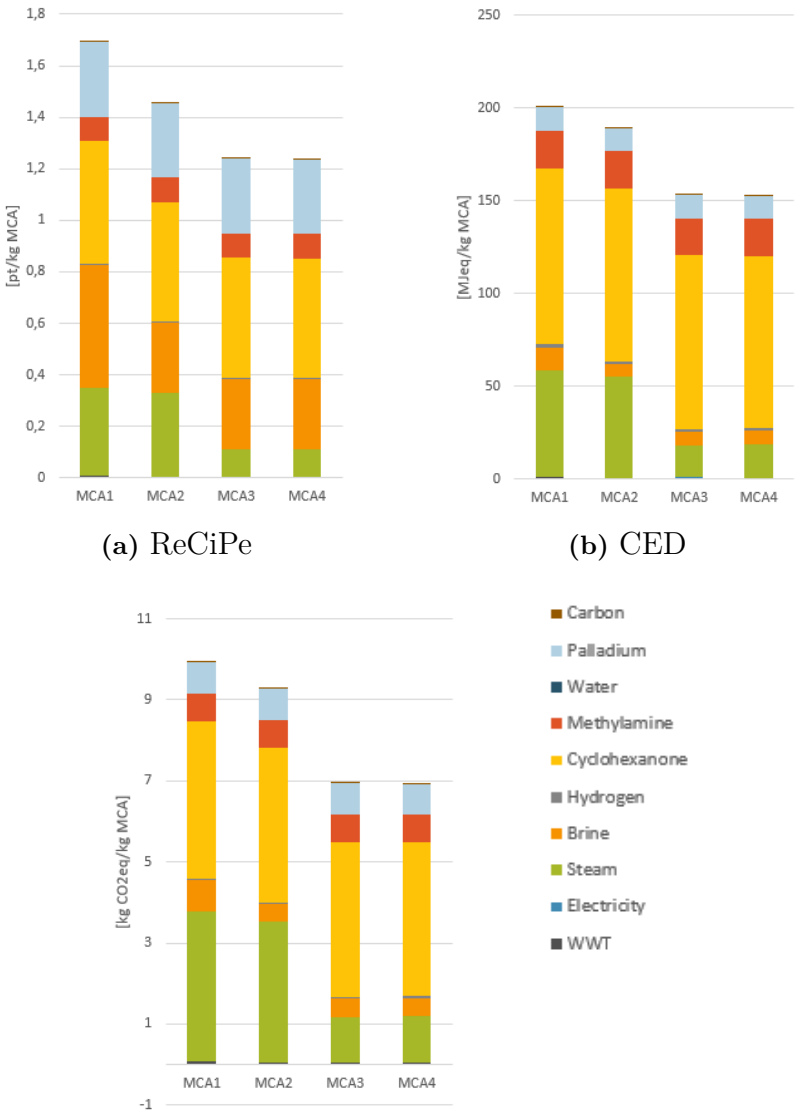

(a) ReCiPe

(b) CED

(c) GWP

Figure 5.4: ReCiPe and CED results for MCA

All MCA models resulted in very similar impacts, with the steam impact being the major difference. MCA_3 and MCA_4, where the optimized distillation pressure was used, the steam demand was significantly lowered, resulting in a smaller impact in all categories. However, the biggest impact for all models and categories comes from the cyclohexanone. Again, the impact from the chemical demands would be hard to reduce, as described earlier.

Similarily to the DMCA results, the WWT, electricity-, and hydrogen demand impacts are close to negligible. In the figures, WWT contains both impact from WWT and the

impact from gaseous waste incineration. Although small, the waste incineration resulted in negative impacts for GWP. This was due to an assumption used in the waste treatment model. It was assumed that the heat recovered from the waste incineration would, in the case of no waste being incinerated, instead be covered by the incineration of oil. The resulting negative impact therefore suggest that the waste incineration gives a lower impact than the corresponding oil incineration would have.

For MCA a palladium-on-carbon catalyst was used (titled Carbon and Palladium in Figure 5.4), where the supporting carbon impact also are almost negligible. However, since palladium is a rare earth metal, its impacts are very high (see Table C.1, Appendix C). For the ReCiPe, the palladium demand results in one of the highest impacts. For CED and GWP, palladium stands for an impact similar to the one from methylamine.

The LCA based on MCA_3 resulted in the highest impact out of the four industrially feasible models (MCA_3 through MCA_6). Therefore, a feasible result range was constructed between the MCA_3 results and the MCA_6 results, and compared to the estimated impact from FineChem in Figure 5.5.

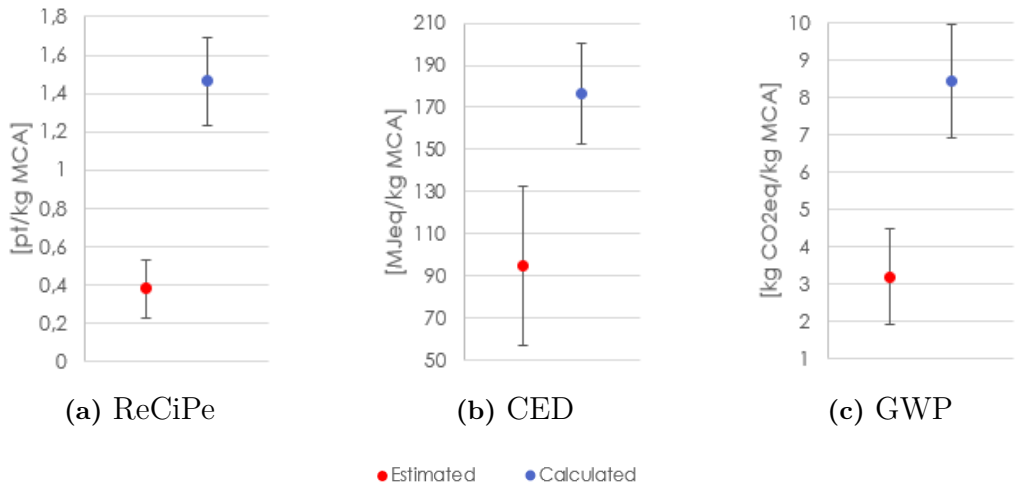

(a) ReCiPe **(b)** CED **(c)** GWP

Figure 5.5: Comparing calculated impacts to estimated impacts for MCA

The comparison shows that the calculated impact ranges are above the estimated ranges for all categories. The FineChem estimation is stated to be best at estimating CED impact [38], and that is also the category where the estimation is the closest to the calculated range.

In Chapter 2.2, the amount of MCA required to capture 1 ton CO_2 was stated. By using the impact of MCA_4 (the model resulting in the lowest impacts), and a solvent make-up of 1.5 kg per ton captured CO_2 (the lower limit of solvent make-up), a lower limit for MCA make-up impact per tonne of CO_2 captured could be calculated. In the same way, the impact from MCA_1 (the model resulting in the highest impacts), and a solvent make-up of 2.5 kg per tonne captured CO_2 (the upper limit of solvent make-up), the upper limit for the impact of MCA make-up per tonne of CO_2 captured was calculated. By using both the calculated impacts, and the FineChem-estimated impacts, two ranges were constructed. The resulting solvent make-up impact ranges and are presented in Table 5.9.

Table 5.9: Impact of MCA make-up per ton of CO_2 captured

	Calculated range	Estimated range
ReCiPe [$pt.ton_{CO_2}^{-1}$]	1.9 - 4.2	0.3 - 1.3
CED [$MJ_{eq}.ton_{CO_2}^{-1}$]	228.6 - 500.5	84.9 - 330.3
GWP [$kg_{CO_2,eq}.ton_{CO_2}^{-1}$]	10.4 - 24.8	2.9 - 11.2

5.2.3 MAPA

The ReCiPe results from the LCA based on $MAPA_3$ through $MAPA_6$ are shown in figure 5.6 a), the CED results in b), and the GWP results in c). The results from $MAPA_1$ and $MAPA_2$ are shown in Appendix C (Chapter C.3).

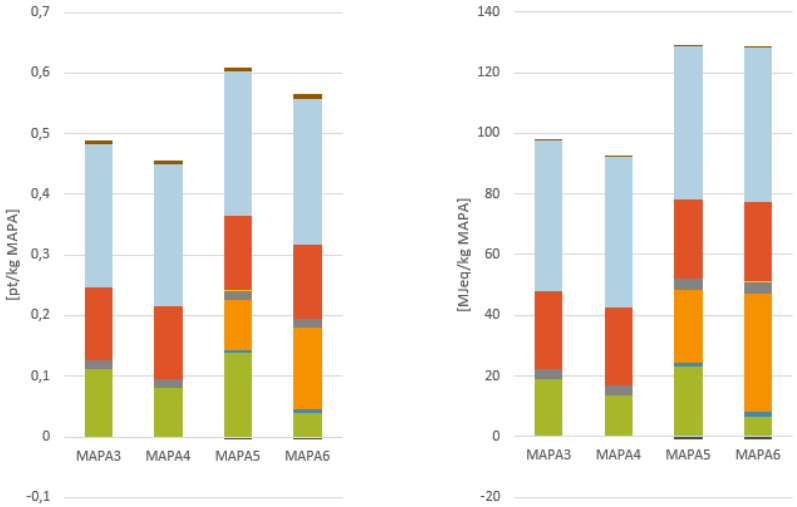

(a) ReCiPe **(b)** CED

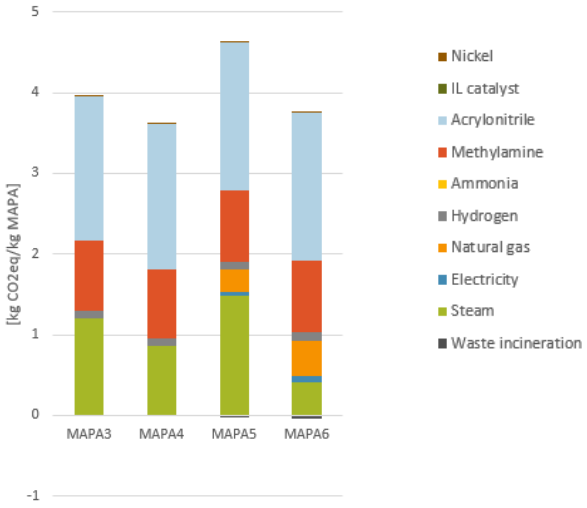

(c) GWP

Figure 5.6: GWP, CED and ReCiPe results for MAPA

The biggest impact for all models comes from the acrylonitrile. The big difference between the models comes from the increased heating demand for the rigorous hydrogenation in $MAPA_5$ and $MAPA_6$. The temperatures required resulted in high impacts because of the use of natural gas-powered fire heating.

Further, the waste incineration needed in $MAPA_5$ and $MAPA_6$ resulted in negative impacts. This was due to the same assumptions described earlier in Chapter 5.2.2. Again, the impact from the reactants would be very hard to decrease. The natural gas demand could be lowered further by adjusting pressures in the models. This however was proven to add a demand for brine instead. It is unclear how big the added brine demand would become. Thus it is possible that an optimal pressure could be reached, where the combined impact from natural gas and brine would be lower than the current natural gas impact. It could also be possible that small adjustments in the model could decrease the steam demand even further. However, the energy requirement details in the models were not investigated further.

The LCA based on $MAPA_3$ resulted in the highest impact out of the four industrially feasible models ($MAPA_3$ through $MAPA_6$). Therefore, a feasible result range was constructed between the $MAPA_3$ results and the $MAPA_4$ results (resulting in the lowest impact), and compared to the impact estimated by the FineChem estimation tool in Figure 5.7.

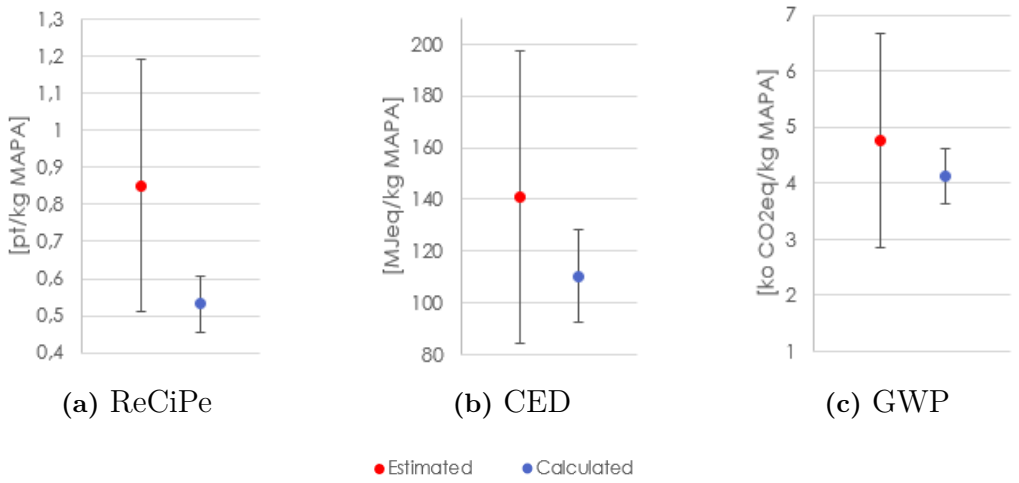

(a) ReCiPe **(b)** CED **(c)** GWP

Figure 5.7: Comparing calculated impact to estimated impacts for MAPA

The comparison shows that the calculated ranges for GWP and CED fit into the lower part of the estimated ranges. The calculated ReCiPe range overlap the bottom of the estimated range, with the lower part below the estimation.

5.2.4 Result comparison

Figure 5.8 show the LCA results for the modelled ranges for ReCiPe, CED and GWP. Estimated and calculated results are shown for DMCA, MCA, MAPA and S1N. Impact data for MEA is also included, taken from Ecoinvent (see Table C.1, Appendix C).

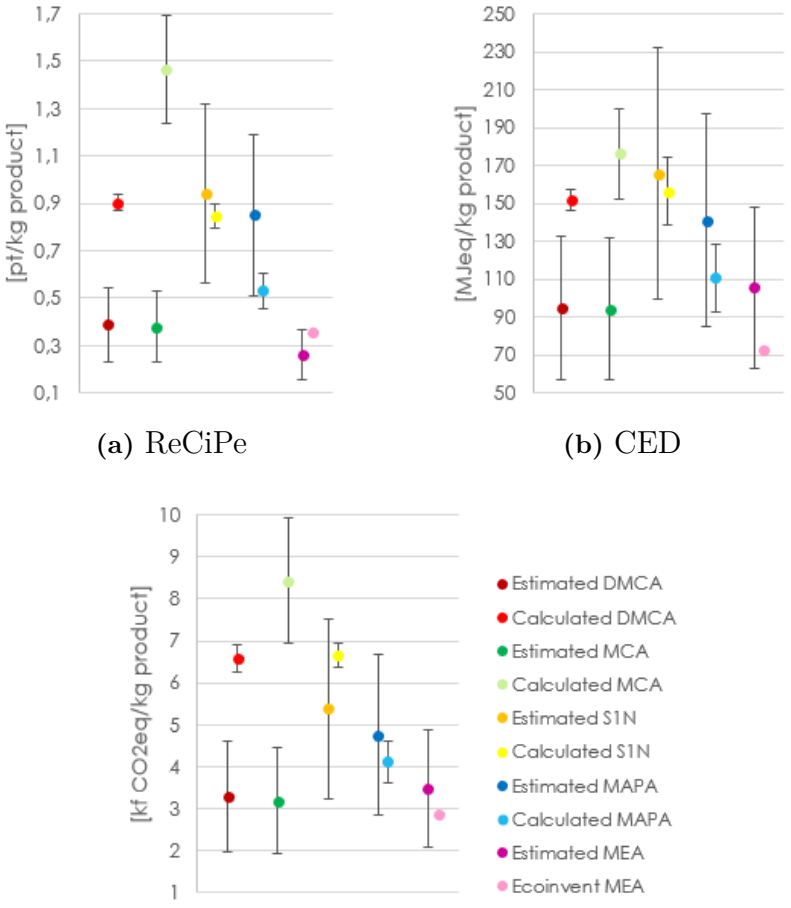

(a) ReCiPe **(b)** CED

(c) GWP

Figure 5.8: Comparing the calculated and estimated impact ranges

For ReCiPe, the highest impact comes from MCA, followed by S1N, DMCA, MAPA and MEA. This differs from the estimated ranges, where S1N gives the highest impact, followed by MAPA, DMCA, MCA and MEA. The same trend can be observed when considering the CED and GWP impact. However, for CED and GWP, the estimated impact for MEA is higher than the estimated impacts for both DMCA and MCA. That both DMCA and MCA presents a big difference between the calculated and estimated range depend on that the same route of synthesis were used in both cases. The result could be tested in the future by using another route of synthesis as a base for the models.

As can be observed, the range for the calculated MCA is wider than the other calculated ranges. This is due to MCA_1 and MCA_2 using atmospheric distillation, and MCA_3 and MCA_4 using the distillation pressure that minimized the heat demand. In all models for the the other compounds, the distillation pressure set to minimize the heat demand was

used. Had the atmospheric distillation not been used for MCA however, the range would have been minimal (see MCA_3 and MCA_4 in Figure 5.4).

These results suggest that the impact for DMCA, MCA and MAPA are far greater than the impact for MEA. However, no data for the CO_2 capture, for the blend of DMCA, MCA and MAPA, was available. To be able to estimate that, data for CO_2 loading, degeneration and such would be necessary. Thus, the impact from carbon capture when using a solvent composed of DMCA, MCA and MAPA could possibly have a smaller impact than when using MEA.

Further, while the calculated impacts sometimes fit into the estimated impact range, it was not always the case. Also, when the calculated range fit into the estimated range, the calculated ranges were always significantly narrower. Along with increased precision, the use of the method enables an overview of the production process, along with a better comprehension of the utility demand. However, the report did not present this in detail. This would however suggest that the calculation method could be worth using, even considering it being time consuming. The FineChem estimation tool only provides a non-interpretable, and sometimes very wide, range.

To further explore the results, the impact, in the form of ReCiPe, of two solvents with hypothetical blends were investigated. The ReCiPe impact of producing one kg of the first solvent, a blend of DMCA, S1N and MAPA, are presented in Figure 5.9. The bottom left corner correspond to a solvent with 100% DMCA, the upper corner correspond to 100% MAPA, and the bottom right corner 100% S1N. The impact ranges from dark blue (small impact) to light yellow (high impact).

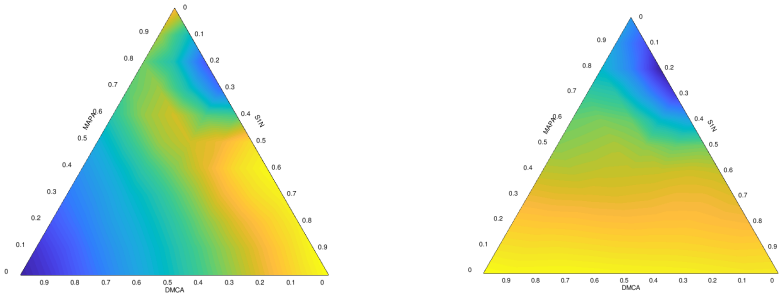

(a) Estimated **(b)** Calculated

Figure 5.9: Comparing calculated ReCiPe to FineChem estimated ReCiPe of a blend of DMCA, S1N and MAPA

The ReCiPe impact of producing one kg of the second solvent, a blend of DMCA, MCA and MAPA, are presented in Figure 5.10. In both figures, the FineChem-estimated impact are shown in a) and the calculated impact shown in b). Only the ReCiPe indicator was explored. The bottom left corner correspond to a solvent with 100% DMCA, the upper corner correspond to 100% MAPA, and the bottom right corner 100% MCA. The impact ranges from dark blue (small impact) to light yellow (high impact), however, both the blue and yellow correspond to higher impacts per kg compared to the first blend in Figure 5.9.

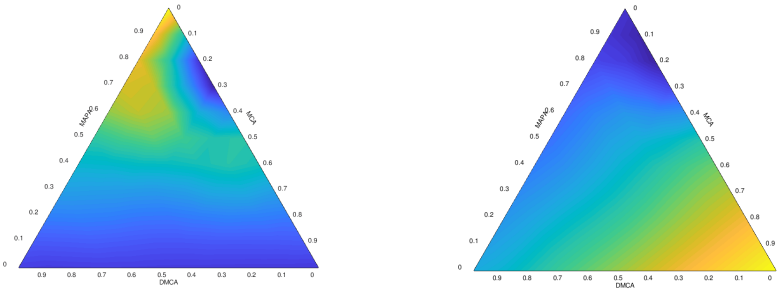

(a) Estimated (b) Calculated

Figure 5.10: Comparing calculated ReCiPe to FineChem estimated ReCiPe of a blend of DMCA, MCA and MAPA

As expected, the FineChem estimated impact for the blends differ from the calculated impact. As can be observed, for the first blend, the smallest calculated impact is given when the blend is made up out of high amounts of MAPA, and small amounts of S1N. The second blend gives the lowest calculated impact when the blend is made up out of high amounts of MAPA, and low amounts of MCA. This was expected since MAPA had the lowest calculated impact out of the four investigated compounds. Overall, the first blend gave the lowest impact per kg of solvent. However, additional data would be required to draw any conclusions about how the blends would perform when absorbing CO_2, and thus the impact from the use of the solvents.

Figure 5.11 shows the impact from the solvent make-up required when capturing 1 ton CO_2, comparing the use of pure MEA and pure MCA as the solvent. The calculated MEA used the impact data from Ecoinvent, multiplied with the higher and lower limit of solvent make-up required during CO_2-capture (see Chapter 2.2), making it a narrow range. The estimated MEA used the estimated range, multiplied with the range of solvent make-up. For MCA, the same ranges are presented above in Table 5.9.

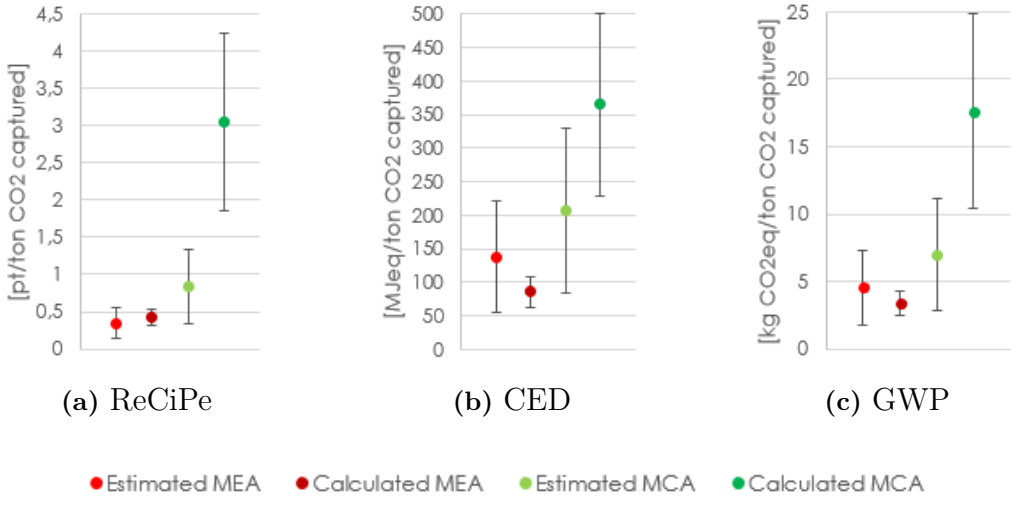

(a) ReCiPe (b) CED (c) GWP

Figure 5.11: Impact of capturing 1 ton CO_2 using MEA or MCA

As can be observed, MCA results in a higher impact than MEA per ton captured CO_2. However, at the same time, MEA have a lower CO_2 loading capacity than MCA. About 45% more solvent is required if the solvent is MEA, compared to MCA, for the capture of one ton CO_2. Although, by only considering the impact for the make-up required during the operation, MEA would be the least environmentally harmful option out of the two.

In the end, in order to match the 1.5 °C-target by the end of the century, according to Figure 5.12, the negative emissions should be of 20 $Gt_{CO_2}.yr^{-1}$ by 2100. Assuming 15 mass% of this amount would be captured using the post combustion CO_2 capture technology with MCA as the solvent, an average of 6 million tonnes of MCA would be required for the solvent make-up in year 2100.

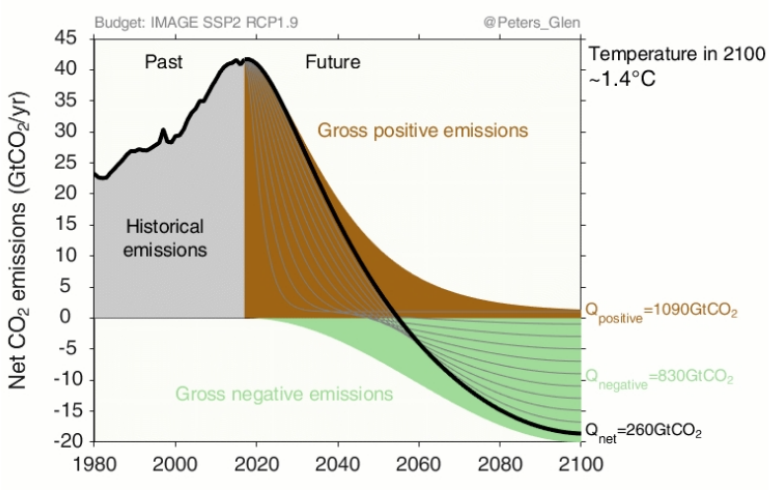

Figure 5.12: Humanity CO_2 emission goal according to SSP2 RCP1.9

Further, the production of the solvents relies on reactants coming from the oil industry. H_2 is today mostly obtained trough steam methane reforming; aniline, acrylonitrile, cyclohexanone and the other reactants also derive from chemical transformation of petroleum compounds. Finding ways not relying on the oil industry to produce the reactants could be an important part in making the production of the CCS solvents more environmentally friendly.

6

Conclusion

The calculated environmental impacts from the hypothetical solvent blend of DMCA, MCA and MAPA are summarized in Table 6.1, also included are the impacts from S1N.

Table 6.1: Summarized environmental impacts of the solvents

	ReCiPe [pt.kg product^{-1}]	CED [MJ_{eq}.kg product^{-1}]	GWP [$kg_{CO_2,eq}$.kg product^{-1}]
DMCA	0.765-0.937	145.97-157.24	6.259-6.989
MCA	1.235-1.691	152.41-200.18	6.932-9.936
MAPA	0.606-0.457	92.637-128.28	3.631-4.607
S1N	0.797-0.895	138.47-174.05	6.371-6.956

The smallest impact came from MAPA, followed by S1N and DMCA, and the highest impact came from MCA. The main part of the environmental impact for all compounds were observed to come from the production of the chemical reactants. However, to be able to draw any conclusion about their environmental impact when used as solvents for CO_2 capture, additional data would be required.

The biggest limitations of this work lies within the routes of synthesis chosen for the modelling. In many cases, no clear route could be found, and the routes chosen might not be the best routes for industrial applications. This uncertainty could be eliminated by making more models, using different routes of synthesis, and thus expanding the impact ranges. However, by doing that, the impact ranges might expand to the extent that the FineChem estimation-ranges would be narrower than the calculated ranges. Without further work however, this cannot be determined.

As mentioned above, more models should be made to increase the sensitivity analyses, along with a more rigorous optimisation of the process parameters. It would also be important in the future to perform techno-economic analyses, as the profitability of the manufacturing processes will more than likely govern the use of the CO_2 extraction solvents.

Further, it would be interesting to assess whether or not there are more environmentally friendly ways to produce the chemical reactants. As mentioned in the results and discussion, as of date, they are mainly produced in the petrochemical industry, and it could be

observed that the major part of the environmental impact came from the reactants.

To conclude, the method used enables an assessment of the environmental impact of non-conventional, non-industrially produced chemicals. The cradle-to-gate LCA gives an understanding of what parts of the production processes are the most environmentally damaging. This makes it possible for producers who would possibly start up an industrial production, to make the right decisions about the process, from an environmental standpoint.

Bibliography

[1] IPCC (Intergovernmental Panel on Climate Change), "Climate Change 2014 Synthesis Report," IPCC (Intergovernmental Panel on Climate Change), Geneva, 2015.

[2] J. G. Olivier, G. Janssen-Maenhout, M. Muntean and J. A. Peters, "Trends in global CO2 emissions: 2013 Report," PBL Netherlands Environmental Assessment Agency Institute for Environment and Sustainability of the European Commission's Joint Research Centre, Hague, 2013.

[3] Center for Climate and Energy Solutions, "Global Emissions," Center for Climate and Energy Solutions, 2017. [Online]. Available: `https://www.c2es.org/content/international-emissions/` [Accessed 28 January 2019].

[4] Global Carbon Capture and Storage Insitute Ltd, "The Global Status of CCS," Global Carbon Capture and Storage Insitute Ltd, Melbourne, 2018.

[5] C. Levêque, "Sustainability assessment of phase-change solvents for CO2 capture - benefits and disadvantages from a sustainability perfective," Chalmers University of Technology, Göteborg, 2018.

[6] J. Gibbins and H. Chalmers, "Carbon capture and storage," Energy Policy, vol. 36, no. 12, pp. 4317-4322, 2008.

[7] B. Xue, Y. Yu, J. Chen, X. Luo and M. Wang, "A comparative study of MEA and DEA for post-combustion CO_2 capture with different process configuration". International Journal of Coal Science and Technology, vol. 4(1), pp. 15-24, 2017.

[8] J. Zhang, "Study on CO2 Capture Using Thermomorphic Biphasic Solvents with Energy-Efficient Regeneration," Technische Universität Dortmund, Dortmund, 2013.

[9] ROLINCAP. (2019). ROLINCAP. Retrieved from `http://www.rolincap-project.eu/` [Accessed 15 May 2019]

[10] J. Davison, P. Freund and A. Smith, "Putting Carbon Back into the Ground," IEA Greenhouse Gas R&D Programme, 2001.

[11] Z. Liang, W. Rongwong, H. Liu, K. Fu, H. Gao, F. Cao, R. Zhang, T. Sema, A. Henni, K. Sumon, D. Nath, D. Gelowitz, W. Srisang, C. Saiwan, A. Benamor, M. Al-Marri, H. Shi, T. Supap, C. Chan, Q. Zhou, M. Abu-Zahra, M. Wilson, W. Olson, R. Idem and P. Tontiwachwuthikul, "Recent progress and new developments in post-combustion carbon-capture technology with amine based solvents," International Journal of Greenhouse Gas Control, vol. 40, pp. 26-54, 2015.

[12] M. Wang, A. Lawal, P. Stephenson, J. Sidders and C. Ramshaw, "Post-combustion CO2 capture with chemical absorbtion: A state-of-the-art review," Chemical Engineering Research and Design, vol. 89, no. 9, pp. 1609-1624, 2011.

[13] H. Lepaumier, D. Picq and P.L. Carrette, "Degradation Study of new solvents for CO2 capture in post-combustion," Energy Procedia, vol. 1, pp. 893-900, 2009.

[14] D.D.D. Pinto, S.A.H. Zaidy, A. Hartono and H.F. Svendsen, "Evaluation of a phase change solvent for CO2 capture: Absorption and desorption tests". International Journal of Greenhouse Gas Control, vol. 28, pp. 318-327, 2014.

[15] S. Badr, "Sustainability Assessment of Amine-based Post Combustion CO2 Capture". Cairo University, 2016.

[16] Global CCS Insitute, (2012). *9.3 RWE/LINDE/BASF Niderausem Pilot Plant*. Available at: `https://hub.globalccsinstitute.com/publications/process-modelling-amine-based-post-combustion-capture-plant-0` [Accessed 25 May 2019].

[17] A. Papadopoulos, I. Tsivintzelis, F. Tzirakis and P. Seferlis, "ROLINCAP Systematic Design and Testing of Advanced Rotating Packed Bed Processes and Phase-Change Solvents for Intensified Post-Combustion CO2 Capture", deliverable 2.1 Database of existing phase-change solvents, published 26/03/2017.

[18] A.F. Ciftja, A. Hartono and H.F. Svendsen, "Experimental study on phase change solvents in CO2 capture by NMR spectroscopy". Chemical Engineering Science, vol. 102, pp. 378-386, 2013.

[19] ChemicalBook, "N,N-Dimethylcyclohexylamine," 2017. [Online]. Available: `https://www.chemicalbook.com/ChemicalProductProperty_EN_CB1854754.html`. [Accessed 30 January 2019].

[20] K. Hayes, "Industrial processes for manufacturing amines," Applied Catalysis A: General, vol. 221, no. 1-2, pp. 187-195, 2001.

[21] P.F. Jackisch, "Process for making cyclic amines". USA Patent 4,521,624, 4 June 1985.

[22] H.F. Efner, "Process for the preparation of secondary and tertiary amines". USA patent 4,954,654, 4 September 1990.

[23] J. Eberhardt, B.W. Hoffer, F. Haese, J-P. Melder, B. Stein, M. Stang, T. Hill and E. Schwab, "Process for preparing an amine", USA patent 2009/0082562 A1, 26 March 2009.

[24] H. Chen (陈洪龄), B. Zhang (张炳庚) and G. Xu (许国平), "Production method for chemical intermediate N-methyl cyclohexylamine", China patent, 1211566A, 1 september 1998.

[25] W. Ji (纪 文 富) and B. Xie (谢 炳 详), "Method of preparing N-methylcyclohexylamine as raw material of bromocaproic hydrochloride medicine", China patent, 1092062A, 10 march 1993.

[26] M. Brezina and P. Zuman, "Reakce karbonylovych sloucenin s aminy V. Polarografická studie reakce cyklanonu s primárními aminy: rovnovázné stavy", Polarograficky ustav Ceskoslovenske akademie ved, Prague, 1952.

[27] X. Jiang, W. Ye, X. Song, W. Ma, X. Lao and R. Shen, "Novel Ionic Liquid with Both Lewis and Bronsted Acid Sites for Michael Addition". International Journal of Molecular Sciences, vol. 12, pp. 7438-7444, 2011.

[28] X. Sun, Y. Du, C. Li and C. Qi, "Novel Efficient Procedure for the Conjugate Addition of Amines to Electron Deficient Alkenes". Kinetics and Catalysis, vol. 51, pp. 653-656, 2010.

[29] A. Fruth, J. Strauss and H. Stuhler, "Process for the preparation of saturated primary fatty amines by hydrogenation of unsaturated fatty acid nitriles". USA patent, 5 175 370, 29 December 1992.

[30] H. Baumann and A-M. Tillman, The Hitch Hiker's Guide to LCA, Lund: Studentlitteratur AB, 2004.

[31] National Institute for Public Health and the Environment. (2018, February 11). RIMV Committed to health and sustainability. Retrieved from LCIA: the ReCiPe model: https://www.rivm.nl/en/life-cycle-assessment-lca/recipe. [Accessed 5 February 2019]
[32] C.D. Noi and A. Ciroth, "Calculation of energy indicators in MJ, LHVs". GreenDelta, 2017.
[33] D. Archer. Global Warming. John Wiley & Sons Ltd, 2012.
[34] J.S. Wilkes, "Properties of ionic liquid solvents for catalysis". Journal of Molecular Catalysis A: Chemical, vol. 214, pp. 11-17, 2004.
[35] Engineering ToolBox, (2007). *Sodium Chloride and Water*. [online] Available at: https://www.engineeringtoolbox.com/sodium-chloride-water-d_1187.html [Accessed 10 May 2019].
[36] Engineering ToolBox, (2005). *Fuel Gas Heating Values*. [online] at: https://www.engineeringtoolbox.com/heating-values-fuel-gases-d_823.html [Accessed 10 May 2019].
[37] A. Kohler, S. Hellwg, E. Recan and K. Hungerbuhler, "Input-Dependent Life-Cycle Inventory Model of Industrial Wastewater-Treatment Process in the Chemical Sector". Environmental Science & Technology, vol. 41, pp. 5515-5522, 2007.
[38] G. Wernet, S. Papadokonstantakis, S. Hellweg and K. Hungerbuler, "Bridging the gaps in environmental assessments: Modeling impacts of fine and basic chemical production". Green Chemistry, vol. 11, pp. 1826, 2009.
[39] Sigma-Aldrich, "Palladium on carbon", (2019). Sigma-Aldrich. [online]. Available at: https://www.sigmaaldrich.com/catalog/product/aldrich/205699?lang=en&region=SE. [Accessed 29 april 2019].

A

Appendix A

This section aims to present the general sequential method used for the sizing of the column. The general method is presented in Figure A.1 below.

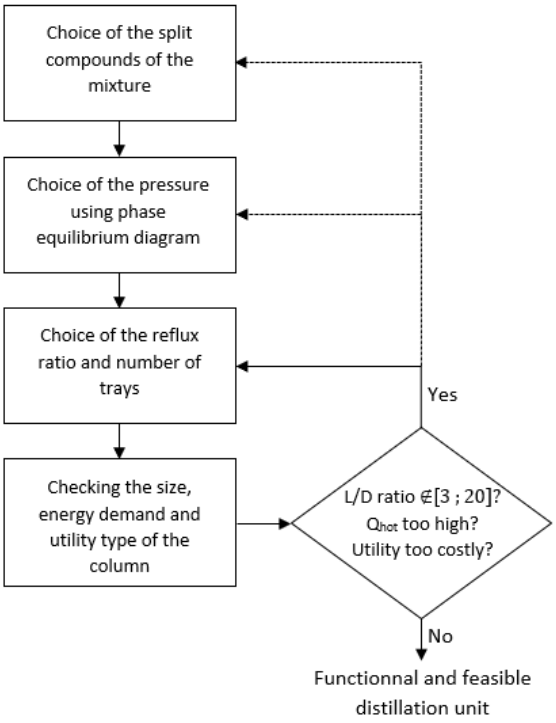

Figure A.1: General methodology used for the synthesis of the distillation units

The first step of the was to choose the split that would occur in the column. This depended on several factors. First, the temperature difference between the potential light key and heavy key (the heavier of the compound to be collected in the distillate and the lighter of the compounds to be gathered in the condensate). The bigger the difference, the easier the separation. The choice of the split also depended on the general objective: the goal was to minimize the energy consumption of the whole process and therefore as little mass as possible should be sent to the distillate of the columns.

Once the split had been fixed, the mixture was approximated to two or three compounds depending on their mass, as it was their separation that would govern the energy demand the most out of all the compounds present in the mixture. In order to explore the impact of the internal pressure of the distillation columns, it was assumed that a range between 0.005-30 bar would be reasonable for industrial columns.

To chose the distillation pressures, the binary or ternary diagrams of these compounds were plotted in Aspen, using pressures inside the chosen range. By choosing the pressure having the larger temperature difference between the dew point and the boiling point curves, thus where the separation would be the easiest under those conditions, that way decreasing the energy requirements of the column. Subsequently, the pressure resulting in the lowest energy requirement was chosen. For all cases this heuristic method was not

completely accurate. In the case of the ternary diagrams, the key parameter observed was the minimum temperature difference between the three boiling points, assuming that a smaller difference induced a more difficult separation, i.e. a more energy requiring separation. One example of such a diagram is presented in Figure A.2.

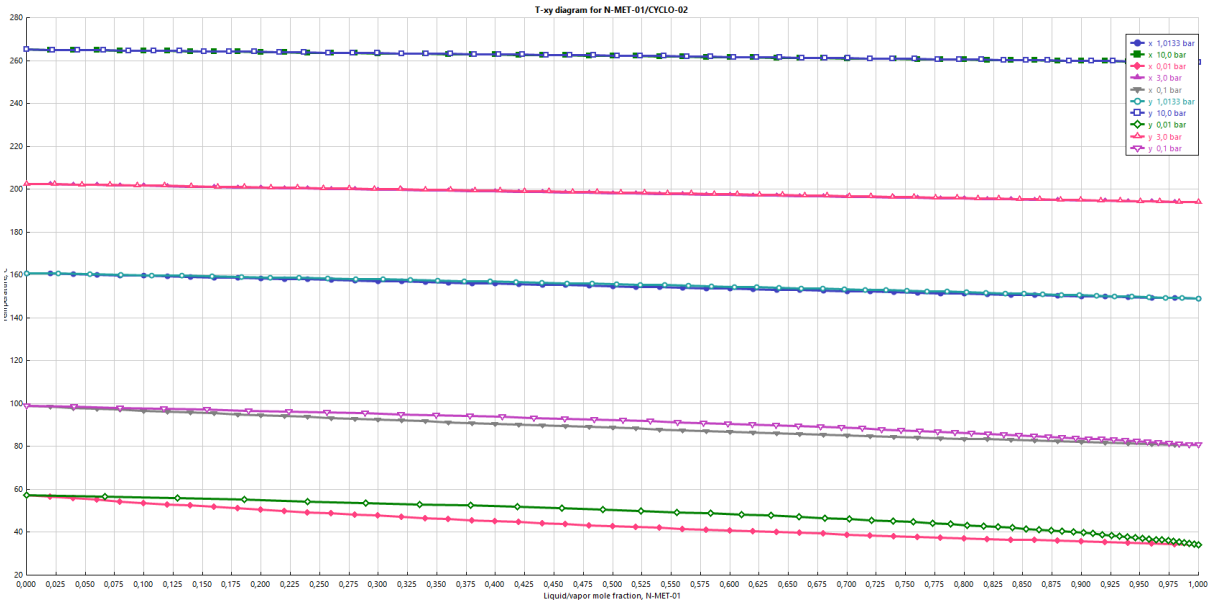

Figure A.2: Binary diagram of DMCA/Cyclohexanol VLE

Furthermore, the column was sized, choosing a suitable number of trays and reflux ratio so that the column was industrially feasible. If some conditions were not fulfilled, lops in the procedure (Figure A.1) were performed, going back one or more steps, until the results were satisfying. The parameters observed were the energy requirement, the impact of the utility required and the size of the column. The size of the column were observed by calculating the distillation ratio

$$3 < \frac{HEPT * N_{trays}}{D} < 20$$

where HEPT was the height of one tray, N_{trays} were the number of trays in the column, and D was the column diameter. When the ratio was found to be bigger than 3, but smaller than 5, it was assumed that in reality the distillation would take place in two parallel distillation columns. If the ratio was found to be smaller than three, several parallel columns would be needed.

This was, however the general method, and all the loops and and the steps was not systematically done. It should be clarified that the column configuration resulting from this procedure was not the optimal one, but rather a functional unit that could be improved with a more computational/systematic approach.

B

Appendix B

The set efficiencies of the compression units in the models are presented in Table B.1. The resulting product flow rate and the purity of the product from all the models for the production of DMCA and MCA are presented in table B.2. The electricity demand in kW and calculated as kWh/kg product from all the models for production of DMCA and MCA are presented in table B.3.

Table B.1: Efficiencies of the compression units

Pump	0.7
Pump driver	0.98
Compressor isentropic efficiency	0.8
Compressor mechanical efficiency	0.95

Table B.2: Product flow rate and purity of product

	[kg.h^{-1}]	[mol%]		[kg.h^{-1}]	[mol%]
DMCA	120.81	99.07	$MAPA_1$	70.57	99.92
MCA_1	375.27	99.10	$MAPA_2$	87.28	99.92
MCA_2	374.36	99.00	$MAPA_3$	70.52	99.93
MCA_3	380.91	99.06	$MAPA_4$	87.27	99.93
MCA_4	385.52	99.02	$MAPA_5$	69.32	99.01
			$MAPA_6$	85.47	99.08

Table B.3: Electricity demand

	[kW]	[kWh.kg$^{-1}_{\text{product}}$]		[kW]	[kWh.kg$^{-1}_{\text{product}}$]
DMCA	10.6021	0.0878	$MAPA_1$	0.0354	0.0005
MCA_1	4.6827	0.0125	$MAPA_2$	0.0438	0.0005
MCA_2	4.6374	0.0121	$MAPA_3$	0.0340	0.0005
MCA_3	4.7727	0.0125	$MAPA_4$	0.0241	0.0005
MCA_4	4.7281	0.0123	$MAPA_5$	8.5868	0.1239
			$MAPA_6$	14.5606	0.1704

The demands for steam in MJ.h^{-1}, the demand for natural gas in MJ.h^{-1} and kg.h^{-1}, and the brine demand in kg.h^{-1}, for all DMCA, MCA and MAPA models are presented in table B.4.

Table B.4: Heating and cooling demand

	Steam [MJ.h^{-1}]	Natural gas [kg.h^{-1}]	Brine [kg.h^{-1}]
DMCA	1862.23	-	202.870
MCA_1	13 814.73	-	2232.43
MCA_2	12 481.22	-	1311.76
MCA_3	4244.10	-	1301.87
MCA_4	4467.07	-	1311.76
$MAPA_1$	18 847.31	-	-
$MAPA_2$	17 873.10	-	-
$MAPA_3$	848.332	-	-
$MAPA_4$	748.724	-	-
$MAPA_5$	1028.65	24.627	-
$MAPA_6$	352.364	49.7	-

The chemical inflow demands in kg.h^{-1} for all DMCA, MCA and MAPA production models are presented in table B.5.

Table B.5: Chemical demands in [kg.h^{-}1]

	DMCA	MCA_1	MCA_2	MCA_3	MCA_4
Acetic acid	3.9258	-	-	-	-
Cyclohexanone	98.1448	343	342.692	343	342.6920
Dimethylamine	44.1570	-	-	-	-
Hydrogen	1.9477	6.9974	6.9286	6.9974	6.9286
Methylamine	-	105	107.838	105	107.8280
Water	6.6657	31.6143	32.4419	31.6277	32.4419

	$MAPA_1$	$MAPA_2$	$MAPA_3$	$MAPA_4$	$MAPA_5$	$MAPA_6$
Acrolyintrile	63.6763	63.6763	42.4511	52.5341	42.4516	52.5341
Ammonia	-	-	-	-	0.1863	0.2355
Ethyl acetate	552.215	368.142	-	-	-	-
Hydrogen	3.2261	3.9928	3.2265	3.9927	3.2899	4.0729
Methylamine	24.8436	31.0574	24.8460	30.7469	24.8460	30.7469

The chemical recovery in mol% for all DMCA, MCA and MAPA production models are presented in Table B.6.

Table B.6: Reactant recovery in mol%

		DMCA	MCA_1	MCA_2	MCA_3	MCA_4	
Cyclohexanone	[%]	94.0	94.1	96.4	95.5	96.7	
Dimethylamine	[%]	96.0	-	-	-	-	
Hydrogen	[%]	97.3	94.8	97.9	96.1	98.2	
Methylamine	[%]	-	97.3	97.0	98.7	97.3	
		$MAPA_1$	$MAPA_2$	$MAPA_3$	$MAPA_4$	$MAPA_5$	$MAPA_6$
Acrylonitrile	[%]	99.9	82.5	99.9	99.9	96.3	96.1
Hydrogen	[%]	99.9	99.9	99.9	99.9	94.4	94.1
Methylamine	[%]	66.7	99.0	99.9	99.9	96.3	96.1

C

Appendix C

C.1 Life Cycle Inventory Data

All impact data as it was taken from Ecoinvent v.3.4 for all utilities, chemicals and catalysts are presented in table C.1, there it is also stated if the data is European or global.

Table C.1: Impact data from EcoInvent v.3.4

		*	ReCiPe total (H.A) [pt.$^{*-1}$]	CED non-renewable [$MJ_{eq}.^{*-1}$]	GWP (100a) [$kg_{CO_2,eq}.^{*-1}$]
Electricity	Europe	[kWh]	0.039	10.9	0.44
Steam	Europe	[MJ]	0.0094	1.56	0.1
Brine	Global	[kg]	0.0187	2.099	0.13
Natural gas		[kg]	0.2313	67.032	0.7565
Acetic acid	Global	[kg]	0.24	52.2	1.73
Acrylonitrile		[kg]	0.39	82.87	2.99
Ammonia	Europe	[kg]	0.23	42.42	2.04
Aniline		[kg]	0.6	100.82	5.4
Cyclohexanone	Europe	[kg]	0.52	104.12	4.26542
Dimethylamine	Europe	[kg]	0.34	77.83	2.3
Ethyl acetate	Global	[kg]	0.36	74.24	2.71
Hydrogen	Europe	[kg]	0.32	79.13	2.07
Methylamine	Europe	[kg]	0.34	72.46	2.45
Tap water	Europe	[kg]	0.000038	0.0071	0.00038
Carbon		[kg]	0.34	81.5	1.88
Copper		[kg]	3.46	167.5	7.91
Iron sulfate	Global	[kg]	0.03	4.34	0.3
Nickel		[kg]	5.28	156.92	11.33
Palladium		[kg]	2 882.17	122 849.4	7 672.28

The estimated waste treatment impacts from the DMCA, MCA and MAPA production models are presented in table C.2. $MAPA_3$ and $MAPA_4$ did not produce any waste streams.

Table C.2: Estimated waste treatment impacts

	ReCiPe total (H.A) [$pt.h^{-1}$]	CED non-renewable [$MJ_{eq}.h^{-1}$]	GWP (100a) [$kg_{CO_2,eq}.h^{-1}$]
DMCA	0.6925	91.3400	9.5871
MCA_1	2.4626	348.8302	32.1914
MCA_2	1.4087	199.4512	18.4173
MCA_3	1.7093	242.1003	22.3558
MCA_4	1.2540	177.5267	16.39723
$MAPA_1$	-135.9540	-32 051.30	-853.6728
$MAPA_2$	-89.9531	-21 207.33	-565.7446
$MAPA_5$	-0.2413	-57.5099	-1.9376
$MAPA_6$	-0.3564	-86.0747	-2.7484

In the models, all waste streams were added together. The composition of these waste streams in all DMCA, MCA and MAPA production models are presented in table C.3.

Table C.3: Waste stream composition in [$kg.h^{-1}$]

	DMCA	MCA_1	MCA_2	MCA_3	MCA_4
Acetic acid	3.8164	-	-	-	-
Cyclohexanone	3.4301	0.8717	2.7352	0.0281	2.7801
Cycohexanol	0.0133	9.8442	-	10.3965	-
Dimethylamine	0.7511	-	-	-	-
DMCA	0.6106	-	-	-	-
Hydrogen	0.1641	0.0142	0.0138	0.0142	0.0138
MCA	-	7.8326	7.2521	2.4627	6.0438
Methylamine	-	0.6733	1.2960	0.6733	1.2961
Water	23.9511	92.1136	94.2384	92.1409	94.2424

	$MAPA_1$	$MAPA_2$	$MAPA_5$	$MAPA_6$
Acrylonitrile	21.2299	11.1429	0.0008	0.0011
Ammonia	-	-	0.4134	0.5165
Ethyl acetate	464.5554	309.7010	-	-
Hydrogen	-	-	0.0645	0.0814
MAPA	-	-	0.5058	0.8209
Diamine *	-	-	0.4742	0.7014
Methylamine	0.0008	0.3106	-	-
Intermediate nitrile	0.0018	0.000002	-	-

* A diamine produced as a byproduct in the hydrogenation to form MAPA

The calculated catalyst make-up flow rate demand in kg/kg product for all DMCA and MCA production models are presented in table C.4.

Table C.4: Calculated catalyst make-up demand per kg product

	Carbon [kg.h^{-1}]	Palladium [kg.h^{-1}]	IL catalyst [kg.h^{-1}]	Nickel [kg.h^{-1}]
DMCA	-	0.0072	-	-
MCA_1	4.8128	0.5348	-	-
MCA_2	4.8128	0.5348	-	-
MCA_3	4.8128	0.5348	-	-
MCA_4	4.8128	0.5348	-	-
$MAPA_1$	-	-	0.0019	0.0960
$MAPA_2$	-	-	0.0019	0.1188
$MAPA_3$	-	-	0.0019	0.0960
$MAPA_4$	-	-	0.0019	0.1188
$MAPA_5$	-	-	0.0019	0.0960
$MAPA_6$	-	-	0.0019	0.1188

C.2 Life Cycle Impact Assessment

The calculated ReCiPe, CED and GWP impacts from all demands, as well as the total impact, for the DMCA production models are presented in table C.5.

Table C.5: Impact per kg produced DMCA

	ReCiPe [$pt.kg^{-1}_{DMCA}$]	CED [$MJ_{eq}.kg^{-1}_{DMCA}$]	GWP [$kg_{CO_2,eq}.kg^{-1}_{DMCA}$]
Electricity	0.0034	0.9566	0.0386
Steam	0.1444	24.0466	1.5415
Brine	0.1338	3.5248	0.2183
Acetic acid	0.0078	1.6963	0.0562
Cyclohexanone	0.4224	84.5860	3.4652
Dimethylamine	0.1243	28.4475	0.8407
Hydrogen	0.0052	1.2757	0.0334
Tap water	0.000002	0.0004	0.00002
Copper	0.0250	1.2090	0.0571
Waste incineration	0.0057	0.7561	0.0794
Total	0.8721	146.4989	6.3303

The calculated impact from the reflux ratio sensitivity analysis, using reflux ratio 30 and 50, are presented in Table C.6. The resulting total impact from the models when using the different reflux ratios are also presented.

	ReCiPe [$pt.kg^{-1}_{MCA}$]	CED [$MJ_{eq}.kg^{-1}_{MCA}$]	GWP [$kg_{CO_2,eq}.kg^{-1}_{MCA}$]
Reflux ratio 30			
Steam	0.1323	22.0215	1.4116
Total	0.8688	145.9707	6.2590
Reflux ratio 50			
Steam	0.2017	33.5861	2.1530
Total	0.9365	157.2417	6.9888

Table C.6: Resulting impacts from the sensitivity analysis

The calculated ReCiPe, CED and GWP impacts from all demands, as well as the total impact, for the four MCA production models are presented in Table C.7. The corresponding impacts for the MAPA production models are presented in Table C.8.

Table C.7: Impact per kg produced MCA

	ReCiPe, total (H.A) [pt.kg_{MCA}^{-1}]		CED, non-renewable [$MJ_{eq}.kg_{MCA}^{-1}$]		GWP (100a) [$kg_{CO_2,eq}.kg_{MCA}^{-1}$]	
	MCA_1	MCA_2	MCA_1	MCA_2	MCA_1	MCA_2
Electricity	0.0005	0.0005	0.1360	0.1315	0.0055	0.0053
Steam	0.3449	0.3258	57.4233	54.2493	3.6810	3.4775
Brine	0.4741	0.2720	12.4866	7.1635	0.7733	0.4437
Cyclohexanone	0.4753	0.4636	95.1659	92.8324	3.8986	3.8030
Methylamine	0.0951	0.0954	20.2741	20.3279	0.6855	0.6873
Hydrogen	0.0060	0.0058	1.4755	1.4264	0.0386	0.0373
Water	0.000003	0.000003	0.0006	0.0006	0.00003	0.00003
Carbon	0.00003	0.0003	0.0082	0.0734	0.0002	0.0017
Palladium	0.2882	0.2882	12.2849	12.2849	0.7672	0.7672
Waste incineration	0.0066	0.0037	0.9295	0.5189	0.0858	0.0479
Total	1.6907	1.4553	200.1845	189.0088	9.9357	9.2710
	MCA_3	MCA_4	MCA_3	MCA_4	MCA_3	MCA_4
Electricity	0.0005	0.0005	0.1366	0.1337	0.0055	0.0054
Steam	0.1044	0.1086	17.3817	18.0758	1.1142	1.1587
Brine	0.2724	0.2712	7.1740	7.1420	0.4443	0.4423
Cyclohexanone	0.4683	0.4622	93.7582	92.5527	3.8409	3.7915
Methylamine	0.0937	0.0951	19.9742	20.2666	0.6754	0.6852
Hydrogen	0.0059	0.0058	1.4536	1.4221	0.0380	0.0372
Water	0.000003	0.000003	0.0006	0.0006	0.00003	0.00003
Carbon	0.0003	0.0003	0.0734	0.0734	0.0017	0.0017
Palladium	0.2882	0.2882	12.2849	12.2849	0.7672	0.7672
Waste incineration	0.0045	0.0033	0.6356	0.4605	0.0587	0.0425
Total	1.2382	1.2351	152.8727	152.4122	6.9460	6.9319

Table C.8: Impact per kg produced MAPA

	ReCiPe, total (H.A) [pt.kg^{-1}_{MAPA}]			CED, non-renewable [$MJ_{eq}.kg^{-1}_{MAPA}$]			GWP (100a) [$kg_{CO_2,eq}.kg^{-1}_{MAPA}$]		
	$MAPA_1$	$MAPA_2$	$MAPA_3$	$MAPA_1$	$MAPA_2$	$MAPA_3$	$MAPA_1$	$MAPA_2$	$MAPA_3$
Electricity	0.00002	0.00002	0.00002	0.0055	0.0055	0.0053	0.0002	0.0002	0.0002
Steam	2.5042	1.9188	0.1127	416.9290	319.4507	18.7654	26.7262	20.4776	1.2029
Hydrogen	0.0146	0.0146	0.0146	3.6200	3.6199	3.6202	0.0947	0.0947	0.0947
Methylamine	0.1198	0.1210	0.1198	25.5271	25.7836	25.5283	0.8631	0.8718	0.8632
Acrylonitrile	0.3522	0.2845	0.2348	74.8278	60.4581	49.8832	2.6998	2.1814	1.7998
Ethyl acetate	2.8190	1.5184	-	581.3456	313.1370	-	21.2210	11.4305	-
IL catalyst	0.00001	0.00001	0.00001	0.0019	0.0016	0.0019	0.00009	0.00007	0.00009
Nickel	0.0072	0.0072	0.0072	0.2136	0.2136	0.2136	0.0154	0.0154	0.0154
Waste incineration	-1.9265	-1.0306	-	-454.4998	-242.9771	-	-12.1054	-6.4819	-
Total	3.8906	2.8339	0.4891	647.9706	479.6929	98.0180	39.5152	28.5898	3.9763
	$MAPA_4$	$MAPA_5$	$MAPA_6$	$MAPA_4$	$MAPA_5$	$MAPA_6$	$MAPA_4$	$MAPA_5$	$MAPA_6$
Electricity	0.00002	0.0048	0.0066	0.0053	1.3503	1.8570	0.0002	0.0545	0.0750
Natural gas	-	0.0822	0.1345	-	23.8158	38.9802	-	0.2688	0.4399
Steam	0.0804	0.1389	0.0386	13.3836	23.1281	6.4316	0.8579	1.4826	0.4123
Hydrogen	0.0146	0.0152	0.0152	3.6202	3.7558	3.7709	0.0947	0.0982	0.0986
Ammonia	-	0.0006	0.0006	-	0.1140	0.1169	-	0.0055	0.0056
Methylamine	0.1198	0.1219	0.1223	25.5285	25.9732	26.0679	0.8632	0.8782	0.8814
Acrylonitrile	0.2348	0.2389	0.2397	49.8844	50.7532	50.9383	1.7999	1.8312	1.8379
IL catalyst	0.00001	0.00001	0.00001	0.0016	0.0020	0.0016	0.00007	0.00009	0.00007
Nickel	0.0072	0.0073	0.0073	0.2136	0.2173	0.2181	0.0154	0.0157	0.0157
Waste incineration	-	-0.0035	-0.0042	-	-0.8297	-1.0071	-	-0.0280	-0.0322
Total	0.4568	0.6063	0.5609	92.6372	128.2799	127.3755	3.6314	4.6068	3.7344

C.3 LCA Results

Figure C.1 shows the LCA results for $MAPA_1$ and $MAPA_2$.

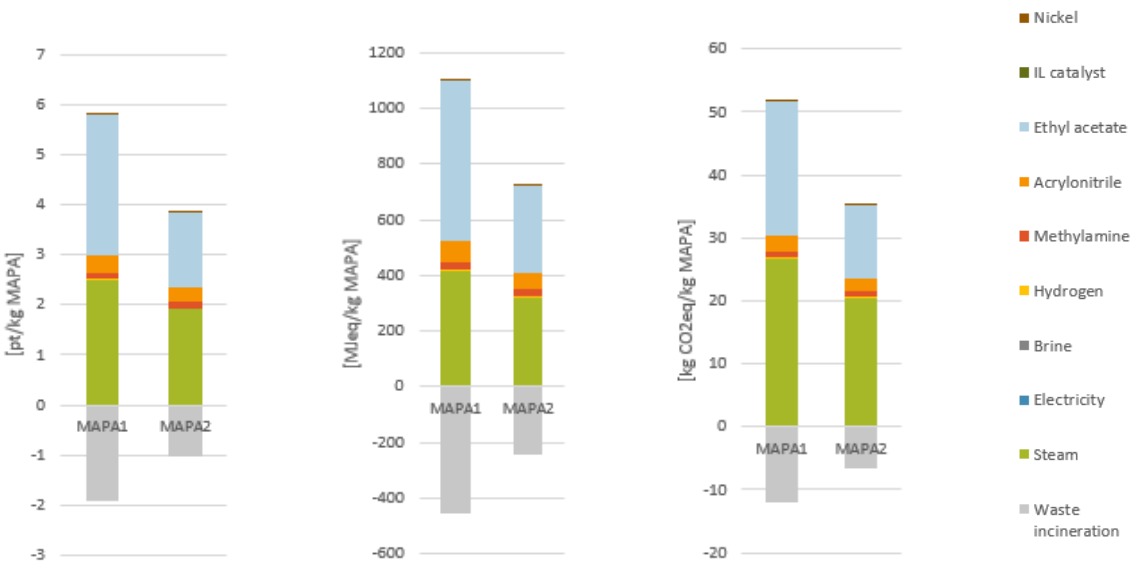

(a) ReCiPe **(b)** CED **(c)** GWP

Figure C.1: LCA results for $MAPA_1$ and $MAPA_2$

D

Appendix D - Confidential

This appendix is not included in this version of the report, due to the confidentiality.

E

Appendix E - Confidential

This appendix is not included in this version of the report, due to the confidentiality.

F

Appendix F - Confidential

This appendix is not included in this version of the report, due to the confidentiality.